

การวิเคราะห์สมรรถนะของเครื่องปฏิกรณ์แบบเชื้อเพลิงผ่านที่เกิดปฏิกิริยาออกโทเทอร์มัลสำหรับการผลิต  
ไฮโดรเจนจากมีเทน



นางสาวมนัสนันท์ วสุสิวรรณ

สถาบันวิทยบริการ

จุฬาลงกรณ์มหาวิทยาลัย

วิทยานิพนธ์นี้เป็นส่วนหนึ่งของการศึกษาตามหลักสูตรปริญญาวิศวกรรมศาสตรมหาบัณฑิต

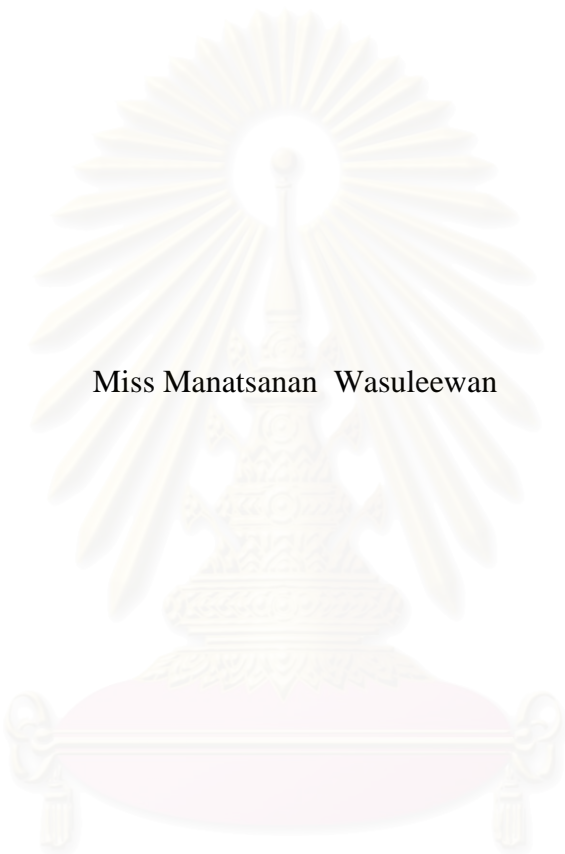
สาขาวิชาวิศวกรรมเคมี ภาควิชาวิศวกรรมเคมี

คณะวิศวกรรมศาสตร์ จุฬาลงกรณ์มหาวิทยาลัย

ปีการศึกษา 2550

ลิขสิทธิ์ของจุฬาลงกรณ์มหาวิทยาลัย

PERFORMANCE ANALYSIS OF AN AUTOTHERMAL MEMBRANE REACTOR FOR  
HYDROGEN PRODUCTION FROM METHANE



Miss Manatsanan Wasuleewan

สถาบันวิทยบริการ  
A Thesis Submitted in Partial Fulfillment of the Requirements  
for the Degree of Master of Engineering Program in Chemical Engineering

Department of Chemical Engineering

Faculty of Engineering

Chulalongkorn University

Academic Year 2007

Copyright of Chulalongkorn University



มนัสนันท์ วสุสิววรรณ : การวิเคราะห์สมรรถนะของเครื่องปฏิกรณ์แบบเยื่อเลือกผ่านที่เกิดปฏิกิริยาออกโตเทอร์มัลสำหรับการผลิตไฮโดรเจนจากมีเทน. (PERFORMANCE ANALYSIS OF AN AUTOTHERMAL MEMBRANE REACTOR FOR HYDROGEN PRODUCTION FROM METHANE) อ. ที่ปรึกษา: ผศ.ดร. อมรชัย อภรณ์วิชานพ, 79 หน้า.

ในงานวิจัยนี้ได้ศึกษาเครื่องปฏิกรณ์รีฟอร์มมิงแบบออกโตเทอร์มัลซึ่งรวมปฏิกิริยารีฟอร์มมิงด้วยไอน้ำและปฏิกิริยาออกซิเดชันเข้าด้วยกันสำหรับการผลิตไฮโดรเจนจากมีเทน ภายในเครื่องปฏิกรณ์แบบออกโตเทอร์มัล ความร้อนจากปฏิกิริยาออกซิเดชันจะถูกใช้สำหรับปฏิกิริยารีฟอร์มมิงด้วยไอน้ำ โดยทั่วไปเครื่องปฏิกรณ์ที่เกิดปฏิกิริยาออกโตเทอร์มัลจะเป็นเครื่องปฏิกรณ์แบบเบดคงที่ที่มีตัวเร่งปฏิกิริยา 2 ชนิดสำหรับปฏิกิริยาออกซิเดชันและปฏิกิริยารีฟอร์มมิงผสมกัน อย่างไรก็ตามเครื่องปฏิกรณ์แบบนี้จะมีปัญหาเกี่ยวกับการจัดการด้านพลังงานความร้อนของทั้งสองปฏิกิริยา งานวิจัยนี้จะศึกษาสมรรถนะของเครื่องปฏิกรณ์ออกโตเทอร์มัล 3 ประเภท ได้แก่ เครื่องปฏิกรณ์แบบเบดคงที่ที่มีตัวเร่งปฏิกิริยาผสมกัน เครื่องปฏิกรณ์ที่แยกตัวเร่งปฏิกิริยาออกเป็น 2 เบด และเครื่องปฏิกรณ์แบบเยื่อเลือกผ่าน โดยใช้แบบจำลองหนึ่งมิติและมีเฟสเดียวที่สภาวะอุณหภูมิก่อเกิดปฏิกิริยาไม่คงที่ สำหรับเครื่องปฏิกรณ์แบบเยื่อเลือกผ่านจะเลือกใช้เยื่อเลือกผ่านชนิดต่างๆ ได้แก่ เยื่อเลือกผ่านไฮโดรเจน เยื่อเลือกผ่านออกซิเจน และเยื่อเลือกผ่านไฮโดรเจนและออกซิเจน ผลของสภาวะในการดำเนินงานที่มีต่อประสิทธิภาพของเครื่องปฏิกรณ์จะถูกวิเคราะห์ในแง่ของค่าการเปลี่ยนของมีเทน ผลได้ของไฮโดรเจนต่อคาร์บอนมอนอกไซด์ ผลได้ของไฮโดรเจนและแฟกเตอร์การเลือกผ่าน ผลการจำลองแสดงให้เห็นว่าเครื่องปฏิกรณ์แบบเยื่อเลือกผ่านไฮโดรเจนและออกซิเจนให้สมรรถนะที่ดีเนื่องจากทำให้ค่าการเปลี่ยนมีเทนเพิ่มขึ้นและลดปัญหาการเกิดจุกครึ้น

ภาควิชา.....วิศวกรรมเคมี.....  
สาขาวิชา.....วิศวกรรมเคมี.....  
ปีการศึกษา.....2550.....

ลายมือชื่อนิสิต..... น.ส. มงโสภาภัทร์ จุลฉัตรรัตน์.....  
ลายมือชื่ออาจารย์ที่ปรึกษา..... อมรชัย อภรณ์วิชานพ.....

# # 4970646921 : MAJOR CHEMICAL ENGINEERING

KEY WORD : AUTOTHERMAL REFORMING / HYDROGEN PRODUCTION /  
MEMBRANE REACTOR / METHANE

MANATSANAN WASULEEWAN: PERFORMANCE ANALYSIS OF AN  
AUTOTHERMAL MEMBRANE REACTOR FOR HYDROGEN PRODUCTION  
FROM METHANE. THESIS ADVISOR: ASST. PROF. AMORNCHAI  
ARPORNWICHANOP, D. Eng., 79 pp.

An autothermal reforming reactor in which the couple of steam reforming with partial oxidation reforming carried out is studied for the production of hydrogen from methane. In the autothermal reforming reactor, the endothermic heat and part of the steam required for steam reforming are balanced by an exothermic oxidation. The autothermal reforming reactor is generally an adiabatic fixed-bed reactor in the presence of mixture of two different catalysts for partial oxidation and steam reforming reactions. However, with such a reactor configuration, the management of the heat integration of the two reactions is difficult. In this work, the performance of three different methane autothermal reforming reactors, i.e., a conventional reactor, a dual-bed reactor and membrane reactor is investigated by using a one-dimensional homogeneous and non-isothermal model. For the membrane reactor, different type of membrane, i.e., H<sub>2</sub>-selective membrane, O<sub>2</sub>-selective membrane and H<sub>2</sub>-O<sub>2</sub> selective membrane, is applied. Effect of various operating parameters on the efficiency of each reactor is evaluated in terms of methane conversion, H<sub>2</sub>/CO of product, hydrogen recovery yield and separation factor. Simulation results show that the H<sub>2</sub>-O<sub>2</sub> selective membrane reactor provides the best performance in terms of the increased methane conversion and the reduced hot spot problem.

Department.....Chemical Engineering...

Field of study...Chemical Engineering...

Academic year.....2007.....

Student's signature.....Manatsanan Wasuleewan

Advisor's signature.....Amornchai Arpornwichanop

## ACKNOWLEDGEMENTS

The author would like to express her sincere gratitude and appreciation to her advisor, Assistant Professor Amornchai Arpornwichanop, for his supervision, invaluable suggestions and discussion throughout the course of this Master Degree study. Furthermore, the author would also be grateful to Associate Professor Sutthichai Assabumrungrat, Dr. Soorathep Kheawhom and Assistant Professor Worapon Kiatkittipong for serving as the chairman and member of thesis committee, respectively.

Financial supports from the Thailand Research Fund (TRF-Master Research Grants) and the Energy Research Institute and the Graduate School of Chulalongkorn University are gratefully acknowledged.

The author would also like to thank all members of Control and Systems Engineering Research Center for their friendship and support over the years of her study.

Special thanks go to Mr. Supattadis Yamniyom and his family for kind suggestions, support, encouragement and everything throughout this study.

Finally, the author would like to express her highest gratitude to her family who always pay attention to her all the times for suggestions, encouragement and financial support throughout this study. The most success of graduation is devoted to her family.

# CONTENTS

	PAGE
<b>ABSTRACT IN THAI</b> .....	<b>iv</b>
<b>ABSTRACT IN ENGLISH</b> .....	<b>v</b>
<b>ACKNOWLEDGEMENTS</b> .....	<b>vi</b>
<b>CONTENTS</b> .....	<b>vii</b>
<b>LIST OF TABLES</b> .....	<b>x</b>
<b>LIST OF FIGURES</b> .....	<b>xi</b>
<b>NOMENCLATURES</b> .....	<b>xiv</b>
 <b>CHAPTER</b>	
<b>I INTRODUCTION</b> .....	<b>1</b>
1.1 Research objective .....	3
1.2 Scopes of research.....	3
1.3 Thesis outline .....	4
<b>II LITERATURE REVIEWS</b> .....	<b>5</b>
2.1 Hydrogen production by autothermal reforming .....	5
2.2 Design of autothermal reformers .....	8
2.3 Membrane reactor for hydrogen production .....	10
<b>III THEORY</b> .....	<b>16</b>
3.1 Autothermal reforming of methane.....	16
3.2 Kinetic rate expressions .....	17
3.3 Membrane reactor .....	21

CHAPTER	PAGE
3.3.1 H <sub>2</sub> -selective membrane .....	22
3.3.2 O <sub>2</sub> -selective membrane .....	22
<b>IV MATHEMATICAL MODEL OF AUTOHERMAL REACTORS.....</b>	<b>24</b>
4.1 Configuration of autothermal reactor.....	24
4.2 Mathematic model of autothermal reactor .....	26
4.2.1 Material balance.....	27
4.2.2 Energy balance.....	28
4.3 Reactor performance .....	30
<b>V SIMULATION RESULTS AND DISCUSSION.....</b>	<b>32</b>
5.1 Model validation .....	32
5.2 Simulation results of a conventional autothermal reactor.....	32
5.2.1 Effect of H <sub>2</sub> O/CH <sub>4</sub> ratio.....	36
5.2.2 Effect of O <sub>2</sub> /CH <sub>4</sub> ratio.....	38
5.2.3 Effect of feed position of steam .....	40
5.3 Simulation results of a dual bed autothermal reactor.....	41
5.3.1 Effect of H <sub>2</sub> O/CH <sub>4</sub> ratio .....	43
5.3.2 Effect of O <sub>2</sub> /CH <sub>4</sub> ratio.....	44
5.4 Simulation results of an autothermal membrane reactor .....	45
5.4.1 H <sub>2</sub> -selective membrane reactor .....	45
5.4.1.1 Effect of H <sub>2</sub> O/CH <sub>4</sub> ratio .....	49
5.4.1.2 Effect of O <sub>2</sub> /CH <sub>4</sub> ratio.....	50
5.4.1.3 Effect of membrane thickness.....	52



CHAPTER	PAGE
5.4.1.4 Effect of operation mode .....	53
5.4.2 O <sub>2</sub> -selective membrane reactor .....	54
5.4.2.1 Effect of H <sub>2</sub> O/CH <sub>4</sub> ratio .....	56
5.4.2.2 Effect of O <sub>2</sub> /CH <sub>4</sub> ratio .....	57
5.4.2.3 Effect of the thickness of O <sub>2</sub> -selective membrane .....	57
5.4.3 H <sub>2</sub> -O <sub>2</sub> selective membrane reactor .....	59
5.4.3.1 Effect of H <sub>2</sub> O/CH <sub>4</sub> ratio .....	61
5.4.3.2 Effect of O <sub>2</sub> /CH <sub>4</sub> ratio .....	63
5.4.3.3 Effect of air pressure .....	64
5.4.3.4 Effect of air temperature .....	65
<b>VI CONCLUSION AND RECOMMENDATIONS.....</b>	<b>67</b>
6.1 Conventional autothermal reactor .....	67
6.2 Dual bed autothermal reactor .....	68
6.3 Autothermal membrane reactors .....	68
6.1.1 H <sub>2</sub> -selective membrane reactor .....	68
6.1.2 O <sub>2</sub> -selective membrane reactor .....	69
6.1.3 H <sub>2</sub> -O <sub>2</sub> selective membrane reactor .....	70
6.4 Recommendations .....	71
<b>REFERENCES.....</b>	<b>72</b>
<b>APPENDIX.....</b>	<b>77</b>
Appendix A .....	78
<b>VITA .....</b>	<b>79</b>

## LIST OF TABLES

		PAGE
<b>Table 3.1</b>	Arrhenius kinetic parameters .....	19
<b>Table 3.2</b>	The equilibrium constant of reactions.....	20
<b>Table 3.3</b>	Van't Hoff parameters for the expression .....	20
<b>Table 3.4</b>	The effectiveness factor of reactions.....	20
<b>Table 5.1</b>	Comparison of simulation results of a conventional autothermal reactor with industrial data (Groote and Froment, 1996) .....	33
<b>Table 5.2</b>	Parameters of a conventional autothermal reactor .....	34
<b>Table 5.3</b>	The effect of H <sub>2</sub> O/CH <sub>4</sub> on reactor performance at O <sub>2</sub> /CH <sub>4</sub> ratio of 0.5.....	36
<b>Table 5.4</b>	The effect of O <sub>2</sub> /CH <sub>4</sub> on reactor performance at H <sub>2</sub> O/CH <sub>4</sub> ratio of 1.5.....	38
<b>Table 5.5</b>	Simulation results of adding steam at different location of the conventional reactor.....	40
<b>Table 5.6</b>	Comparison of simulation results between conventional and dual bed autothermal reactors by varying the H <sub>2</sub> O/CH <sub>4</sub> ratio .....	43
<b>Table 5.7</b>	Comparison of simulation results between conventional and dual bed autothermal reactor in case of varying O <sub>2</sub> /CH <sub>4</sub> ratio .....	44
<b>Table 5.8</b>	Parameters of H <sub>2</sub> -selective autothermal membrane reactor.....	45
<b>Table 5.9</b>	Parameters of O <sub>2</sub> -selective autothermal membrane reactor.....	54
<b>Table 5.10</b>	Effect of the H <sub>2</sub> O/CH <sub>4</sub> ratio and the O <sub>2</sub> /CH <sub>4</sub> ratio on the H <sub>2</sub> /CO ratio of product in O <sub>2</sub> -selective membrane reactor .....	57

## LIST OF FIGURES

		PAGE
<b>Figure 4.1</b>	Conventional autothermal reactor for hydrogen production .....	24
<b>Figure 4.2</b>	Autothermal membrane reactor (a) H <sub>2</sub> membrane reactor (b) O <sub>2</sub> membrane reactor .....	25
<b>Figure 4.3</b>	Autothermal H <sub>2</sub> -O <sub>2</sub> membrane reactor .....	25
<b>Figure 4.4</b>	Dual bed autothermal reforming reactor .....	26
<b>Figure 5.1</b>	The temperature profile of a conventional autothermal reactor .....	34
<b>Figure 5.2</b>	The methane conversion profile of a conventional autothermal reactor .....	35
<b>Figure 5.3</b>	The composition profile of components in a conventional autothermal reactor .....	35
<b>Figure 5.4</b>	The temperature profile of a conventional reactor by varying H <sub>2</sub> O/CH <sub>4</sub> ratio .....	37
<b>Figure 5.5</b>	Methane conversion profile of a conventional reactor by varying H <sub>2</sub> O/CH <sub>4</sub> ratio .....	37
<b>Figure 5.6</b>	The temperature profile of a conventional reactor by varying O <sub>2</sub> /CH <sub>4</sub> ratio .....	39
<b>Figure 5.7</b>	Methane conversion profile of a conventional reactor by varying O <sub>2</sub> /CH <sub>4</sub> ratio .....	39
<b>Figure 5.8</b>	The temperature profile of a conventional and dual bed reactor .....	42
<b>Figure 5.9</b>	Methane conversion profile of a conventional and dual bed reactor .....	42
<b>Figure 5.10</b>	Temperature profile of a H <sub>2</sub> -selective membrane reactor .....	46

<b>Figure 5.11</b>	Methane conversion profile of a H <sub>2</sub> -selective membrane reactor .....	47
<b>Figure 5.12</b>	Mole fraction profile of synthesis gas from H <sub>2</sub> -selective membrane reactor .....	47
<b>Figure 5.13</b>	Hydrogen separation factor and hydrogen recovery yield profile of a H <sub>2</sub> -selective membrane reactor .....	48
<b>Figure 5.14</b>	CH <sub>4</sub> conversion and gas temperature outlet by varying H <sub>2</sub> O/CH <sub>4</sub> ratio.....	49
<b>Figure 5.15</b>	Hydrogen separation factor and recovery yield by varying H <sub>2</sub> O/CH <sub>4</sub> ratio .....	50
<b>Figure 5.16</b>	CH <sub>4</sub> conversion and gas temperature outlet by varying O <sub>2</sub> /CH <sub>4</sub> ratio.....	51
<b>Figure 5.17</b>	Hydrogen separation factor and recovery yield by varying O <sub>2</sub> /CH <sub>4</sub> ratio.....	51
<b>Figure 5.18</b>	Hydrogen separation factor by varying thickness of H <sub>2</sub> -selective membrane .....	52
<b>Figure 5.19</b>	Composition profile of synthesis gas from H <sub>2</sub> -selective membrane reactor (under vacuum condition) .....	53
<b>Figure 5.20</b>	H <sub>2</sub> separation factor and recovery yield of H <sub>2</sub> -selective membrane reactor (vacuum condition) .....	54
<b>Figure 5.21</b>	Temperature profile of an O <sub>2</sub> -selective membrane reactor .....	55
<b>Figure 5.22</b>	Methane conversion profile of an O <sub>2</sub> -selective membrane reactor .....	55
<b>Figure 5.23</b>	Temperature outlet and CH <sub>4</sub> conversion of an O <sub>2</sub> -selective membrane reactor by varying H <sub>2</sub> O/CH <sub>4</sub> ratio .....	56

<b>Figure 5.24</b>	Effect of the $O_2/CH_4$ ratio on an $O_2$ -selective membrane reactor .....	58
<b>Figure 5.25</b>	Effect of membrane thickness on an $O_2$ -selective membrane reactor.....	58
<b>Figure 5.26</b>	Temperature profile of a $H_2-O_2$ selective membrane reactor .....	59
<b>Figure 5.27</b>	Methane conversion profile of a $H_2-O_2$ selective membrane reactor.....	60
<b>Figure 5.28</b>	Gas composition profile of $H_2-O_2$ selective membrane reactor .....	60
<b>Figure 5.29</b>	The hydrogen recovery yield profile of a $H_2-O_2$ selective membrane reactor .....	61
<b>Figure 5.30</b>	Effect of $H_2O/CH_4$ ratio on outlet temperature and methane conversion of an $H_2-O_2$ selective membrane reactor .....	62
<b>Figure 5.31</b>	Effect of $H_2O/CH_4$ ratio on $H_2$ separation factor and recovery yield of a $H_2-O_2$ selective membrane reactor .....	62
<b>Figure 5.32</b>	Effect of $O_2/CH_4$ ratio on the performance of a $H_2-O_2$ selective membrane reactor .....	63
<b>Figure 5.33</b>	Effect of $O_2/CH_4$ ratio on the $H_2$ separation factor and recovery yield of a $H_2-O_2$ selective membrane reactor .....	64
<b>Figure 5.34</b>	Effect of air pressure on the performance of a $H_2-O_2$ selective membrane reactor .....	65
<b>Figure 5.35</b>	The $CH_4$ conversion and $H_2$ recovery yield of $H_2-O_2$ selective membrane reactor by varying air temperature .....	66

## NOMENCLATURES

- $A$  = Cross section area of reactor ( $m^2$ )
- $A_{m,H_2}$  =  $H_2$ -selective membrane area per unit length ( $m^2/m$ )
- $A_{m,O_2}$  =  $O_2$ -selective membrane area per unit length ( $m^2/m$ )
- $Cp_i$  = Heat capacity of component i ( $J/mol K$ )
- $Ea_j$  = Activation energy of reaction j ( $J/mol$ )
- $E_{A,H_2}$  = The apparent activation energy of  $H_2$ -selective membrane ( $kJ/mol$ )
- $E_{A,O_2}$  = The apparent activation energy of  $O_2$ -selective membrane ( $kJ/mol$ )
- $J_{H_2}$  = Permeability of hydrogen ( $mol/m^2 s$ )
- $J_{O_2}$  = Permeability of oxygen ( $mol/m^2 s$ )
- $k_j$  = The rate constant of reactions j ( $mol/kg s$ )
- $k_m$  = Average thermal conductivity ( $J/m K s$ )
- $k_{oj}$  = The pre-exponential factor of rate constant for reactions j ( $mol/kg s$ )
- $Keq_j$  = The equilibrium constant of reactions j
- $K_i$  = The adsorption coefficient of component i
- $K_i^0$  = The adsorption coefficient of component i for oxidation reaction
- $K_{oi}$  = The Van't Hoff parameters of component i
- $n_i$  = Mole of component i ( $mol$ )

- $p_i$  = Partial pressure of component i (bar)
- $P_{m,H_2}$  = Pre-exponential factor of the H<sub>2</sub>-selective membrane (mol m/bar<sup>0.5</sup>m<sup>2</sup>s)
- $P_{m,O_2}$  = Pre-exponential factor of the O<sub>2</sub>-selective membrane (mol/m K s)
- $q_{H_2}$  = Heat flux between tube and shell side of H<sub>2</sub>-selective membrane (J/s)
- $q_{O_2}$  = Heat flux between tube and shell side of O<sub>2</sub>-selective membrane (J/s)
- $r_j$  = Reaction rate of reaction j (mol/kg s)
- $R$  = The universal gas constant (J/mol K)
- $T$  = Temperature (K)
- $T_{tube}$  = Temperature inside the tube (K)
- $T_{shell}$  = Temperature inside the shell (K)
- $\bar{T}$  = Average temperature of the membrane (K)
- $x_m$  = Thickness of membrane tube (m)
- $Y_{H_2, recovery}$  = Hydrogen recovery yield (mole H<sub>2</sub>/mole CH<sub>2</sub>)

### GREEK LETTERS

- $\eta_j$  = The effectiveness factor of reactions j
- $\varepsilon$  = Void of catalyst bed
- $\rho_{cat}$  = Density of catalyst (kg/m<sup>3</sup>)
- $\delta_{H_2}$  = The thickness of H<sub>2</sub>-selective membrane layer (m)

$\delta_{O_2}$  = The thickness of O<sub>2</sub>-selective membrane layer (m)

$\alpha_{H_2}$  = Hydrogen separation factor (-)

$\Delta H_{ads,i}$  = Adsorption heat of components i

$\Delta H_{r,j}^0$  = Heat of reactions j (J/mol)

$\Delta H_{H_2}$  = The heat transferred by permeating H<sub>2</sub> from tube to shell side (J/mol)

$\Delta H_{O_2}$  = The heat transferred by permeating O<sub>2</sub> from tube to shell side (J/mol)

## SUBSCRIPTS

*cat* = Catalyst

*CH<sub>4</sub>* = Methane

*CO* = Carbon monoxide

*CO<sub>2</sub>* = Carbon dioxide

*H<sub>2</sub>* = Hydrogen

*H<sub>2</sub>O* = Steam

*N<sub>2</sub>* = Nitrogen

*O<sub>2</sub>* = Oxygen

*r* = Reaction

## ACRONYM

ACR = Autothermal cyclic reforming



ATR = Autothermal reforming

A/F = Air-to-fuel ratio

CAR = Gas heated reforming

CPO = Catalytic partial oxidation

CRM = Methane combined reforming

GHSV = Gas hourly space velocity

H<sub>2</sub>/CO = Hydrogen-to-carbon monoxide ratio

H<sub>2</sub>O/CH<sub>4</sub> = Steam-to-methane ratio

O<sub>2</sub>/CH<sub>4</sub> = Oxygen-to-methane ratio

POX = Partial oxidation

PrOx = Preferential oxidation reactor

SRM = Conventional steam reforming

W/F = Water-to-fuel ratio

สถาบันวิทยบริการ  
จุฬาลงกรณ์มหาวิทยาลัย

# CHAPTER I

## INTRODUCTION

Hydrogen is considered as one of the most promising energy carriers that will replace the use of the fossil fuel in the future. Besides its direct use as automotive fuel, hydrogen can be efficiently converted into many useful energy forms. One of the most attractive hydrogen technologies is fuel cell, an electrochemical device that converting the chemical energy of a fuel into electricity.

However, a major obstacle for hydrogen energy system is the lack of hydrogen supply in the energy carrier form. In general, hydrogen can be prepared by different methods and from various sources. A reforming process is the most widely used technology for hydrogen production. Among the various types of hydrocarbon fuels fed to a reformer, i.e., methane, methanol and ethanol, methane as the major component of natural gas, is a convenient feedstock because the existing natural gas pipeline infrastructure makes it readily available and accessible at any point along the distributed chain.

There are three most commercially developed methods to reform fuel. These are steam reforming, partial oxidation and autothermal reforming. Although steam reforming provides the highest hydrogen yield compared with other reforming processes, it involves a highly endothermic reaction and thus, requires external heat input. The external heat needed to drive the reaction is often provided by combustion of a fraction of the incoming natural gas feedstock (up to 25%) (Ogden, 2001) and heat transfer to the reactants is accomplished indirectly through a heat exchanger. For the partial oxidation process, hydrocarbon feed is oxidized with oxygen less than the stoichiometric ratio, such that incomplete combustion products, carbon monoxide and hydrogen, are formed. This reaction is mildly exothermic and no indirect heat exchanger is needed; however, it gives lower hydrogen yield. Recently, the number of researches has focused on the autothermal reforming process by coupling of steam

reforming with partial oxidation reforming as a potential alternative. The endothermic heat and part of the steam required for steam reforming are balanced by exothermic oxidation.

The concept of autothermal operations has recently increased attention as an approach for optimizing heat balance. In general, the standard design of an autothermal reactor for moderately exothermic reactions requires an adiabatic fixed-bed reactor connected with a heat exchanger so that the hot reactor effluent heats up the cold feed to the required reaction temperature. This can be done in a separate heat exchanger or by partial or total integration of the heat exchanger into the reactor. For highly endothermic processes such as steam reforming, low temperature heat produced from reactor effluents is insufficient for heating up the feed to the required high temperature for the endothermic reaction. To overcome this difficulty, the autothermal coupling of exothermic and endothermic reactions in a single reactor in which the reaction mixture can be used as a heating/cooling medium is introduced. An importance example concerning such a concept is an autothermal reforming reactor (Ersoz *et al.*, 2003; Hoang and Chan, 2004; Hoang *et al.*, 2005; Halabi *et al.*, 2007; Wang H.M., 2007).

There are a number of researches focused on the autothermal reforming of methane for hydrogen production. Most of previous works investigated the effects of different operating parameters such as molar air-to-fuel ratio, the molar water-to-fuel ratio and the flowrate of the feedstock on the reactor performance (Groote and Froment, 1996; Peña *et al.*, 1996; Ersoz *et al.*, 2003; Hoang and Chan, 2004; Hoang *et al.*, 2005; Halabi *et al.*, 2007; Wang H.M., 2007). In order to increase the conversion of fuel, there are a number of researches focused on autothermal membrane reactor for hydrogen production. (Ji *et al.*, 2003; Lattner and Harold, 2004; Basile *et al.*, 2005; Charudatta *et al.*, 2005; Tiemersma *et al.*, 2005) An autothermal reforming reactor is generally an adiabatic fixed-bed reactor in the presence of mixture of two different catalysts for partial oxidation and steam reforming reactions. However, with this reactor configuration, the management of heat integration of the two reactions is difficult.

In this work, we investigate the performance of three different methane autothermal reforming reactors, i.e., a conventional reactor, a dual bed reactor and a membrane reactor. In the dual bed autothermal reactor, the catalyst bed is divided into two zones; the first zone involves the partial oxidation whereas the second zone involves the steam reforming. For the membrane reactor, different types of membrane, i.e., H<sub>2</sub>-selective membrane, O<sub>2</sub>-selective membrane and H<sub>2</sub>-O<sub>2</sub> membrane are applied. Simulations are performed based on a one-dimensional homogenous model and non-isothermal model. Effect of various operating parameters on the efficiency of each reactor is evaluated in terms of methane conversion, H<sub>2</sub>/CO of product, hydrogen recovery yield and hydrogen separation factor.

## 1.1 Research Objective

The objective of this study is to investigate the performance of three autothermal reactors, i.e., a conventional reactor, a dual bed reactor and a membrane reactor with different membrane type for the production of hydrogen from methane. The effect of operating parameters on reactor performance in terms of methane conversion, hydrogen-to-carbon monoxide ratio, hydrogen recovery yield and hydrogen separation factor is investigated.

## 1.2 Scopes of research

In this study, three different types of an autothermal reforming reactor for hydrogen production from methane are investigated. First, a conventional reactor in which the reaction side is packed with Ni-MgAl<sub>2</sub>O<sub>4</sub> catalyst (Xu and Froment, 1989) is considered. Secondly, a dual bed reactor in which the reaction part is separated into two sections is studied. The first section of the dual bed reactor is the oxidation section in which Pt-Al<sub>2</sub>O<sub>3</sub> catalyst is packed (Trimm and Lam, 1980) whereas the second one involves a steam reforming reaction and is packed with Ni-MgAl<sub>2</sub>O<sub>4</sub> catalyst. Finally, a membrane reactor with different membrane types, i.e., H<sub>2</sub>-selective membrane, O<sub>2</sub>-selective membrane, and H<sub>2</sub>-O<sub>2</sub> selective membrane, is studied. In the H<sub>2</sub>-selective membrane reactor (Pd-Ag membrane), hydrogen can permeate from the reaction side to a permeate side for pure hydrogen production whereas in the O<sub>2</sub>-

selective membrane (perovskite membrane), oxygen from air can permeate from the non-reaction side to the reaction side to react with methane in feed stream. For the H<sub>2</sub>-O<sub>2</sub> selective membrane reactor, the reactor configuration considered consists of a double jacket tube of two membranes.

To analyze the reactor performances, the influences of operating parameters, i.e., thickness of membranes, pressure and temperature of the permeation side on methane conversion, outlet gas temperature, hydrogen recovery yield and hydrogen separation factor are considered under steady state and non-isothermal conditions.

### **1.3 Thesis Outline**

This thesis is organized as follows: First, the literature reviews related to hydrogen production by autothermal reforming, design of autothermal reactors and membrane reactors for hydrogen production are presented in Chapter II. In Chapter III, basic theory of autothermal reforming, kinetic rate expression and membrane reactor are explained. Next, the configuration and mathematic models which are based on material and energy balances of the autothermal reactor are presented in Chapter IV. The simulation results of the conventional, dual bed and membrane reactors are presented in Chapter V. Finally, the conclusions and the recommendations for future work are given in Chapter VI.

## CHAPTER II

### LITERATURE REVIEWS

Hydrogen is an important substance in chemical, refinery and petrochemical industries. There is an increasing interest in the utilization of hydrogen as an energy carrier because it creates almost no pollution; for example, hydrogen or hydrogen-rich gas is used as fuel in proton exchange membrane fuel cells. In general, hydrogen can be produced by a number of reforming processes, i.e., steam reforming, partial oxidation and autothermal reforming process. However, the autothermal reforming process has attracted much research attention as it couples endothermic and exothermic reactions. This chapter provides a review of the advance and development in autothermal reformer and membrane reactor for hydrogen production.

#### 2.1 Hydrogen production by autothermal reforming

The autothermal reforming has received much attention in research during recent years because it combines the effects of both the endothermic steam reforming and the exothermic partial oxidation by feeding fuel, air and steam into reactor. The autothermal reforming has major advantages of lower energy requirement and lower process temperature than other reforming.

The performance of different processes for the production of synthesis gas from methane such as conventional steam reforming (SRM), partial oxidation (POX), autothermal reforming (ATR), methane combined reforming (CRM), gas heated reforming (CAR) and catalytic partial oxidation (CPO) are compared (Peña *et al.*, 1996). The consumption of raw fuels and energy, investments and operating costs are considered. The result indicated the ATR plant offered lower costs of about 18% with respect to the SRM.

Groote and Froment (1996) proposed the modeling and simulation of reactors for the catalytic partial oxidation of natural gas to synthesis gas. The steam reforming reactions and water-gas shift reaction are parallel or more or less consecutive to the total combustion, depending upon the degree of reduction of the catalyst, which is determined by the temperature and the gas phase composition. The calculation of the net rates of coke formation was included in the simulation. The influence of carbon dioxide and steam was also investigated.

Hoang and Chan (2004) presented a two-dimensional reformer model of catalytic autothermal reforming of methane for hydrogen production. The model is developed to simulate the conversion behavior of the reformer and covered chemical kinetics and heat and mass transfer phenomena in the reformer. Results showed that the performance of the reformer is dependent on the molar air-to-fuel ratio (A/F), molar water-to-fuel ratio (W/F), and the space velocity of the feedstock mixture. Later, Hoang *et al.* (2005) investigated the effect of molar air-to-fuel ratio (A/F), the molar water-to-fuel ratio (W/F) and the flowrate of the feedstock mixture on catalytic autothermal reforming of methane for hydrogen production over a sulfide nickel catalyst on a gamma alumina support. The optimum conditions for high methane conversion and high hydrogen yield are  $A/F = 3-3.5$ ,  $W/F = 2-2.5$  and a fuel flow rate below  $120-250 \text{ l h}^{-1}$ . Under these conditions, a methane conversion of 95–99% and a hydrogen yield of 39–41% on a dry basis can be achieved and 1 mole of methane can produce 1.8 moles of hydrogen at an equilibrium reactor temperature of not exceeding  $850 \text{ }^\circ\text{C}$ .

Also, Halabi *et al.* (2007) studied the autothermal reforming process of methane in a fixed bed reformer for hydrogen production. The process is simulated using a 1-D heterogeneous reactor model under small-scale of dynamic and steady state conditions. The influence of temperatures of gas feed and catalyst bed, oxygen/carbon and steam/carbon ratios, gas hourly space velocity (GHSV), and feed contaminations on gas temperature, methane conversion, hydrogen yield and purity, and reforming efficiency is investigated. An optimal operational window of a GHSV range from 1050 to  $14,000 \text{ h}^{-1}$ , steam/carbon molar ratio of 4.5–6.0, and oxygen/carbon molar ratio of 0.45–0.55 is obtained to achieve a high conversion of

93%, hydrogen purity of 73% on dry basis, thermal reformer efficiency of 78%, and a yield of 2.6 mole hydrogen per 1 mole of methane fed.

Then, Wang (2008) studied on the hydrogen generation by methane autothermal reforming method by experiment. The temperature profile along the axis of the reformer was measured and discussed. The peak temperature of the reformer appeared in the part of 1/4 to 2/4 of the reformer length from inlet to outlet. The maximum hydrogen yield, hydrogen mole numbers generated per mole of methane consumed of 2.71, was achieved at molar oxygen-to-carbon ratio of 1.68 and molar steam-to-carbon ratio of 2.5. Under this condition, the energy conversion efficiency of the reforming process reached 81.4% based on the lower heating values.

In addition, Ersoz *et al.* (2003) studied an autothermal reforming process with lower and higher molecular weight hydrocarbon fuel using HYSYS software. The result showed that the selection of the operation parameters is very important as they have an effect on the autothermal reforming efficiency and hydrogen production. Then, Zhixiang *et al.* (2006) studied the autothermal reforming (ATR) process of propane and optimized the operating conditions with PRO/II from SIMSCI for proton exchange membrane fuel cell application. In ATR system including water gas shift and preferential oxidation, heat in hot streams and cold streams is controlled to be balance. Different operation conditions were studied. The result showed that the ATR process with the highest efficiency was chosen with the process parameters: feed temperature was 425<sup>0</sup>C, steam to carbon ratio was 2.08, stoichiometry of air was 0.256.

From the literature reviews, it can be seen that most researches focused on the analysis of the effect of several parameters such as molar air-to-fuel ratio, the molar water-to-fuel ratio and the flowrate of the feedstock mixture on the performance of the autothermal reforming of different feedstock for hydrogen production. Furthermore, a few studies have concerned the design of catalyst bed configuration in an autothermal reactor to improve its performance.



## 2.2 Design of autothermal reformers

The autothermal reforming is the coupling of steam reforming and partial oxidation reforming in the single unit. Therefore, the unit should be compact. The designation of autothermal reformer has been the subject of research interest.

A reactor for autothermal reforming with two different sections is designed by Marsh and Thiagarajan (1992). The methane is oxidized in the upper section, while the steam and dry reforming are carried out in the bottom section. Furthermore, they studied that the selection of high operation pressure and appropriate steam/carbon and hydrogen/carbon values to avoid soot formation.

Ma *et al.* (1996) designed and investigated the performance of a class of adiabatic dual-bed catalytic reactor systems with cylindrical and spherical geometries of the coupling of the oxidation of methanol to the steam reforming reaction. The effect of water-to-methanol feed ratio on hydrogen production yield and methanol conversion. These systems were two coaxial cylindrical systems, two spherical systems and a dual-bed system. These systems may be used to promote internal heat exchange for the coupled reaction network. The result of analysis showed that the coaxial cylindrical systems, and the dual-bed single tubular reactor need optimal water-to-methanol feed ratio about 3-4, while the spherical systems require a ratio less than 1 for equivalent or even better performance.

Avci *et al.* (2001) proposed the study of configuration of catalyst fixed bed reaction system and compared with experimental results reported for a bench scale integral reactor. Reactor operation at different feed ratios is analyzed for both catalyst bed configurations which are a dual-bed and mixed-bed catalyst by simulations. The result showed that these simulations are in agreement with the experimental results reported. The mixed-bed catalyst results higher hydrogen yield and carbon monoxide yield than the dual bed catalyst. Although the dual bed catalyst configuration results low hydrogen yield but very low carbon monoxide yield which can be used as feedstock of PEMFCs. Also, the researches performed by Vernon *et al.* (1992) focused on the effect of the geometry of one step catalytic reactors. They studied the partial oxidation and autothermal reforming process on fixed bed reactors.

Additionally, Fukuhara and Igarashi (2005) designed a wall-type reactor by combining endothermic and exothermic reactions in one reactor. A wall-type reaction system consisted of endothermic and exothermic reaction channels stacked up and a fixed bed reaction system at the same configuration were studied and compared them by numerical simulation. The result showed that the temperature profiles of the simulation in the fixed bed reaction system predicted a hardly controlling the system, for generating a large different in temperature. But in wall type reaction system, the temperature difference in endothermic and exothermic channels was very small and the temperature distribution was almost in line with the set temperature, indicating the effective exchange of the reaction energy by conductive heat transfer. And Sanger *et al.* (2004) proposed the designation of annular integrated reformer which difference being that an extra pre-reforming section was interposed prior to the main reaction and oxidation section. These kinds of designs could help achieve high efficiencies by using waste energy and decreasing the heat loss from the hot spot areas.

Moreover, Dicks (1996) developed a process with separated reactors. The first reactor is dedicated to pre-reforming of inlet fuel by steam, while the residual gases will react with oxygen on monolithic catalyst placed in second reactor. Later, Kumar *et al.* (2003) proposed an autothermal cyclic reforming (ACR) process operated in a three-step cycle that involves steam reforming (step 1) of the fuel in a Ni catalyst bed, heating the catalyst bed via oxidation (step 2) of the Ni catalyst, and finally reducing the catalyst to the metallic state (step 3). In order to produce a continuous stream of hydrogen, at least two reactors were needed to carry on the reforming and regeneration step simultaneously. The ACR process is unique technology that can be applied for hydrogen or synthesis gas production from different fuels without the dilution of nitrogen.

From literature reviews, the development of autothermal reformers focused on various design of the reactor configuration for efficient integration of heat from exothermic partial oxidation and endothermic steam reforming reaction and investigated the influence of several operating parameters on their performance. In addition, many researchers have attended the membrane reactor which combines the separator and the reactor together for improve the performance.

## 2.3 Membrane reactor for hydrogen production

As mentioned earlier, three most commercially developed methods to reform fuel are steam reforming, partial oxidation and autothermal reforming. However, it is known that these reforming reactions are reversible reactions and their conversions are limited by chemical equilibrium. Membrane reactors can be used to overcome this problem as removal of reaction product can improve reaction conversion. As a result, various studies have been carried out on the application of membrane reactor for hydrogen production.

In steam reforming process, Yu *et al.* (2005) studied of system simulation to investigate the performance of a porous ceramic membrane reactor for hydrogen production of methane steam reforming. The results showed that the methane conversions much higher than the corresponding equilibrium values can be achieved in the membrane reactor due to the selective removal of products from the reaction zone. The effects of various process parameters such as the reaction temperature, the reaction side pressure, the feed flow rate and the steam to methane molar feed ratio as well as the sweep gas flow rate and the operation modes, on the behavior of membrane reactor were analyzed and discussed.

Tong and Matsumura (2005) studied the reforming with steam and methane on low temperature to produce hydrogen and carbon dioxide over a commercial nickel catalyst in an equilibrium-shift reactor with an 11- $\mu\text{m}$  thick palladium membrane (Mem-L) on a stainless steel porous metal filter. The methane conversion with the reactor is higher than its equilibrium value without membrane due to the equilibrium-shift combined with separation of pure hydrogen through the membrane. The methane conversion in a reactor with an 8- $\mu\text{m}$  membrane (Mem-H) is similar to that with Mem-L, although the hydrogen permeance through Mem-H is almost double of that through Mem-L.

Yoshida *et al.* (2001) studied numerical and experimental of methane steam reforming in a packed bed type membrane reactor with silica-zirconia porous membrane. Methane conversion of the membrane reactor exceeded the thermodynamic equilibrium value, and puerility of production of hydrogen was

generally above 95% by volume. The model provided good agreement between experimental and theoretical results. In the application of the porous membrane to the membrane reactor, water vapor permeation had a significant influence on the performance of the membrane reactor.

Also, Ohmori *et al.* (2005) studied the effects of membrane properties in terms of permeability and selective permeability on the design parameters of a porous ceramic membrane reactor for hydrogen production in simulation. The design and operating parameters of the membrane reactors associated with four sets of membranes with different permeability were determined to achieve both the hydrogen production rate of 1 m<sup>3</sup>/h (STP) and the recovery efficiency of 80% at 773 K in methane steam reforming. It was found that less membrane area was required when a membrane with higher permeability value was used.

For methanol steam reforming, Lin and Rei (2001) studied the effect of palladium membrane on the conversion of methanol in steam reforming for hydrogen production. The reaction was carried out over Cu/ZnO/Al<sub>2</sub>O<sub>3</sub> catalysts at 350°C. The stability of the catalyst was affected by the composition of Cu, Zn, and Al. The higher the content of Al is the better stability of the catalyst than other. A double-jacketed membrane reactor was used to conduct both reforming and oxidation reactions simultaneously in separate compartments. The heat released from the oxidation part can be directly transferred into the reforming part to compensate the heat required from the external furnace. The measured heat supply was found to be strongly depending on the recovery yield of hydrogen. And Gadhe and Gupta (2005) proposed the reforming of methanol is carried out in supercritical water to produce hydrogen along with carbon monoxide, methane and carbon dioxide. The reactions are catalyzed by the wall of the tubular reactor made of Inconel 600. Experiments are conducted to study the effects of the pressure, residence time, and steam-to-carbon ratio on the H<sub>2</sub> yield. Both the experimental results and equilibrium calculations showed that, as the pressure is increased, methanation of carbon monoxide and carbon dioxide takes place, resulting in a loss of hydrogen. In addition, the methane formation is favored at a high residence time and low steam-to-carbon ratio.

Chen *et al.* (2004) investigated the steam reforming of heptane over nickel-based catalyst in a circulating fluidized bed membrane reformer (CFBMR) at 723-823 K and 101.3-2026 kPa for hydrogen production and carbon monoxide formation. The model is developed to account for the effect of carbon deposition on the overall reforming kinetics. The results showed that the deposited carbon can be efficiently gasified by steam, hydrogen, carbon dioxide, or oxygen in this novel CFBMR, making carbon-free operation practically possible, especially when steam to carbon feed ratio is higher than 2.5. Later in 2006, Chen *et al.*, proposed the steam reforming of liquid hydrocarbons over a self-made nickel catalyst for hydrogen production in a fixed bed palladium membrane reactor (PMR). The applied palladium membrane was developed by a novel electroless plating method. Owing to the selective removal of hydrogen by the membrane, the yield of hydrogen greatly increased; meanwhile the yield of methane efficiently decreased. The purity of hydrogen in the permeate side of membrane could be maintained over 99.5%. The reactions in the steam reforming of liquid hydrocarbons and hydrogen separation are highly integrated in the PMR.

Furthermore, Ferreira-Aparicio *et al.* (2005) designed a palladium membrane reactor to be applied to the dry reforming of methane for pure hydrogen production at a small scale. The parameters affecting the reactor operation were the extraction conditions, the carbon dioxide-to-methane ratio in the reactant mixture composition, and the reactants feed flow rate. The reactant mixtures with carbon dioxide-to-methane ratios close to 2 offered the best results: high hydrogen recovery yields (above 95%) and lower carbon deposition in the catalysts under the severe conditions imposed by the membrane reactor operation. The dispersion of nickel on high oxygen mobility Supports, such as Ce-Zr mixed oxides ( $\text{Ce}_{0.5}\text{Zr}_{0.5}\text{O}_2$ ), which are chemically stable under reaction conditions, results in highly efficient catalysts capable of keeping their Surface free of inactive carbon deposits.

For partial oxidation reforming, Zhu *et al.* (2006) developed a new mixed reforming method for hydrogen production on a dense ceramic membrane  $\text{Ba}_{0.5}\text{Sr}_{0.5}\text{Co}_{0.8}\text{Fe}_{0.2}\text{O}_{3-\delta}$ (BSCFO) with a catalyst  $\text{LiLaNiO}/\gamma\text{-Al}_2\text{O}_3$  in a membrane reactor and reforming a simulated gasoline. During a 500-h long-term test at optimized reaction conditions, all the components in the simulated gasoline converted completely, and around 90% selectivity of carbon monoxide, around 95% selectivity

of hydrogen were achieved. This provides a new optional way of hydrogen production for fuel cells.

Also, Basile *et al.* (2005) investigated the behavior of a dense Pd/Ag membrane reactor (MR) in terms of methanol conversion in oxidative steam reforming as well as hydrogen production. The parameters considered are the operating temperature and the oxygen-to-methanol feed ratio. The experimental results show that the MR gives methanol conversions higher than traditional reactors (TRs) at each temperature investigated. In the later, they studied the steam reforming reaction of methanol (MSR) to produce pure hydrogen in a flat Pd–Ag membrane reactor (MR) (Basile *et al.*, 2006). Investigating the behavior of methanol conversion in the MSR reaction carried out in MR, the influence of methanol feed flow rate, the operating temperature and oxygen-to-methanol feed ratio on the methanol conversion has been studied. Some experimental data concerning methanol conversion have been compared with the literature data.

In addition to the application of membrane reactors for autothermal reforming, Ji *et al* (2003) simulated the H<sub>2</sub> membrane reactor of catalytic partial oxidation process for pure hydrogen production base on thermodynamic analysis by using one-dimensional steady-state heterogeneous model. The simulation and thermodynamic analysis results indicate that increasing the inlet ratio H<sub>2</sub>O/CH<sub>4</sub> cannot enhance the pure H<sub>2</sub> production rate. The pure hydrogen production rate increases with the inlet methane rate increasing. For the same inlet rate of methane, operation the process at higher inlet temperature increases hydrogen production rate. And Ji *et al.*, 2003 simulated O<sub>2</sub> membrane reactor of the conventional catalytic partial oxidation reactor. The output temperature and the mole flow rates of different species in the tube side and the shell side can be calculated. The result showed that the operation of the membrane catalytic partial oxidation reactor is more favorable when the inlet temperature is increased and the operation pressure is decreased from a thermodynamic point of view.

Tiemersma *et al.* (2005) proposed the conceptual feasibility of a packed bed membrane reactor for the methane autothermal reforming for the production of ultrapure hydrogen. The development of a two-dimensional pseudo-homogeneous

packed bed membrane reactor model solves the continuity equations, the momentum equations, the component mass and energy balances. In adiabatic operation, autothermal operation can be achieved. However, large axial temperature excursions were seen at the reactor inlet, which are disadvantageous for membrane life and catalyst performance.

Charudatta *et al.* (2005) studied multifunctional reactor concept for the production of ultrapure hydrogen (carbon monoxide concentration <10 ppm) from methane for online use in downstream polymer electrolyte membrane fuel cells for small-scale applications. They integrated perm-selective palladium metallic membranes for hydrogen removal with selective oxygen addition through dense perovskite membranes. Incorporation of both types of membranes within a single reactor has the advantage of producing ultrapure hydrogen and pure carbon monoxide. The membrane-assisted fluidized-bed reactor consists of a partial oxidation bottom section and a steam reforming/water gas shift top section. Using thermodynamic equilibrium calculations and more detailed fluidized-bed membrane reactor modeling, it is demonstrated that autothermal operation with high methane conversions and hydrogen yields can be achieved with a relatively small catalyst inventory.

Hydrogen production by steam reforming of heptane is investigated in a novel autothermal circulating fluidized bed (CFB) membrane reformer (Chen and Elnashaie, 2005). Pseudo-steady-state simulations show that at high temperatures, the catalyst is not regenerated, the nickel reforming catalyst deactivates quickly. The autothermal operation for the entire adiabatic reaction-regeneration process is achievable when the exothermic heat generated from the catalyst regenerator is sufficient to compensate for the endothermic heat consumed in the riser reformer. For this process autothermal operation is the most efficient.

Lattner and Harold (2004) proposed several reactor types for the autothermal reforming of hydrocarbon fuels for the production of hydrogen in PEM fuel cell systems. Hydrogen perm-selective membrane reactors (Pd-based and proton conducting oxide) are compared to the three-step reactor system consisting of an adiabatic autothermal reforming reactor, cooled water gas shift reactor, and a preferential oxidation (PrOx) reactor. The study utilizes kinetic rate expressions

modified using literature data on the autothermal reforming of *n*-tetradecane. Resulting that the Pd membrane reactor eliminates the need for a separate WGS reactor, as the selective removal of hydrogen enables sufficient hydrogen production and recovery. The overall efficiency of the Pd membrane reactor system is comparable to the conventional system; a small 1% efficiency gain is attributed to elimination of the hydrogen losses associated with the PrOx reactor. Later, Lattner and Harold (2006) proposed the bench-scale fixed-bed reactor for the methanol autothermal reforming under near-adiabatic conditions. The experimentally demonstrated the conversion of methanol to hydrogen over a copper-based catalyst. Axial distribution of air through multiple porous ceramic membranes was used to limit the peak temperature within the catalyst bed. Methanol conversion, product selectivity, and temperature were measured at discrete axial positions as a function of steam-to-carbon ratios, feed temperatures, pressures, and two different air distributor designs. The effect of space velocity was implicitly studied via the axial composition profile measurements while the oxygen-to-carbon ratio was adjusted to achieve an overall methanol conversion exceeding 90%. The system was simulated using an adiabatic one dimensional reactor model comprising kinetic rate expressions of Peppley et al. (1999). Very good agreement between data and model was achieved by assuming the oxidation reaction to be instantaneous (limited by oxygen supply). The results support a phenomenological view that the exothermic oxidation reactions occur in a narrow zone in close proximity to the porous membranes, leaving the bulk of the catalyst between membrane tubes in the reduced state and therefore active for conducting the endothermic reforming reactions.

From literature reviews, the development of autothermal reformers focused on design of the reactor configurations, investigated the influence of several operating parameters and studied the membrane reactor for efficient integration of heat and for improvidence performance of reactor for hydrogen production.

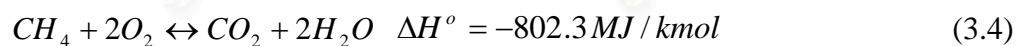
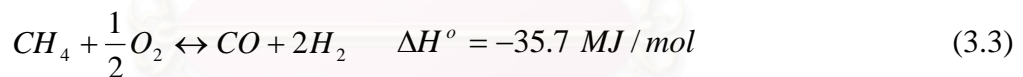
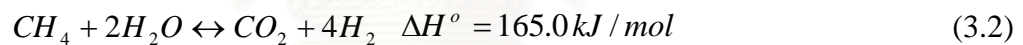
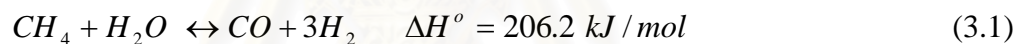


# CHAPTER III

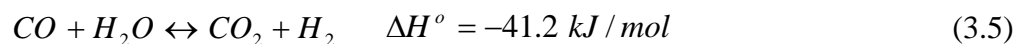
## THEORY

### 3.1 Autothermal reforming of methane

An autothermal reforming process involves exothermic partial oxidation and endothermic steam reforming reactions. A hydrocarbon feed (methane) is reacted with both steam and air to produce hydrogen-rich gas. The main chemical reactions involved in the process are the steam reforming reactions to produce carbon monoxide and carbon dioxide and hydrogen (Equations (3.1)-(3.2)), the partial oxidation reaction (Equation (3.3)), and the total oxidation reaction (Equation (3.4)):



In general, while the steam reforming reactions (Equations (3.1)-(3.2)) is preceded, the synthesis gas produced is further reacted with steam via the water-gas shift reaction (Equation (3.5)) to produce carbon monoxide and hydrogen as shown below:



This reaction is favored at temperature of less than about 600°C, and can take place as low as 200°C with sufficiently active catalysts. The steam reforming reactions (Equations (3.1)-(3.2)) are endothermic and require external heat input.

Methane and steam react in catalyst filled tubes. To avoid coking or carbon build-up on the catalysts, molar ratio of steam-to-carbon should be about 3. It is noted that at lower steam-to-carbon ratio, coke can be produced via Boudard reactions. The favor steam reformer condition is at the pressure of 3-25 atm. and the temperature of 700°C to 850°C.

In the partial oxidation reaction (Equations (3.3)), methane is oxidized with oxygen less than the stoichiometric ratio to product incomplete combustion products, carbon monoxide and hydrogen. When the methane is oxidized with excess amount of oxygen, the reaction becomes catalytic combustion reaction or the complete combustion reaction as shown in Equation (3.4). Although catalysts are not required because of the high temperature operation, the hydrogen yield per mole of methane input can be enhanced by use of catalysts (Loftus, 1994). The partial oxidation reactor is more compact than a steam reformer; in the steam reformer, large heat must be added indirectly via a heat exchanger.

Unlike the steam methane reformer, the autothermal reformer requires no external heat source and no indirect heat exchangers. This makes autothermal reformers simpler and more compact than the steam reformers. In the autothermal reforming, the mixture of methane, air and steam, is fed and the partial oxidation reaction supplies all the heat needed to drive the catalytic steam reforming reactions. Thus, autothermal reformers typically offer higher system efficiency than partial oxidation systems, where excess heat is not easily recovered.

### **3.2 Kinetic rate expressions**

The kinetic rate expressions based on Ni/ $\alpha$ -Al<sub>2</sub>O<sub>3</sub> catalysts for the steam reforming reactions are given by Xu and Froment (1989). This model is considered to be more general and has been tested under lab scale conditions. The following equations are the kinetic rates of methane steam reforming (Equations (3.1) and (3.2)) and water gas shift reaction (Equation (3.5)):

$$r_1 = \frac{\frac{k_1}{p_{H_2}^{2.5}} \left( p_{CH_4} p_{H_2O} - \frac{p_{H_2}^3 p_{CO}}{Keq_1} \right)}{\left( 1 + K_{CO} p_{CO} + K_{H_2} p_{H_2} + K_{CH_4} p_{CH_4} + K_{H_2O} p_{H_2O} / p_{H_2} \right)^2} \quad (3.6)$$

$$r_2 = \frac{\frac{k_2}{p_{H_2}^{3.5}} \left( p_{CH_4} p_{H_2O}^2 - \frac{p_{H_2}^4 p_{CO_2}}{Keq_2} \right)}{\left( 1 + K_{CO} p_{CO} + K_{H_2} p_{H_2} + K_{CH_4} p_{CH_4} + K_{H_2O} p_{H_2O} / p_{H_2} \right)^2} \quad (3.7)$$

$$r_5 = \frac{\frac{k_5}{p_{H_2}} \left( p_{CO} p_{H_2O} - \frac{p_{H_2} p_{CO_2}}{Keq_5} \right)}{\left( 1 + K_{CO} p_{CO} + K_{H_2} p_{H_2} + K_{CH_4} p_{CH_4} + K_{H_2O} p_{H_2O} / p_{H_2} \right)^2} \quad (3.8)$$

For the catalytic combustion of methane (Equations (3.4)), the most common catalysts used for this reaction are based on a metal catalyst. The rate equation associated with the catalytic combustion of methane in the presence of platinum-supported catalyst is given as follows (Trimm and Lam, 1980):

$$r_4 = \frac{k_{4,a} x_{CH_4} x_{O_2}}{\left( 1 + K_{CH_4}^o x_{CH_4} + K_{O_2}^o x_{O_2} \right)^2} \frac{k_{4,b} x_{CH_4} x_{O_2}}{\left( 1 + K_{CH_4}^o x_{CH_4} + K_{O_2}^o x_{O_2} \right)} \quad (3.9)$$

The reaction rate parameters, the Van't Hoff parameters for species adsorption and the equilibrium parameters of the reactions can be expressed as:

$$k_j = k_{oj} \exp \left[ -\frac{Ea_j}{RT} \right] \quad j = 1,2,4,5 \quad (3.10)$$

$$K_i = K_{oi} \exp \left[ -\frac{\Delta H_{ad,j}}{RT} \right] \quad i = CO, CO_2, CH_4, H_2O, O_2 \quad (3.11)$$

$$Keq_j = K_j^o \exp \left[ \frac{-H_j}{T} \right] \quad j = 1,2,4,5 \quad (3.12)$$

where,  $Ea_j$  ( $J/mol$ ) is the activation energy of reactions j.

$\Delta H^o$  ( $kJ/mol$ ) is the heat of reactions j.

$k_j$  ( $mol/kg\ cat.s$ ) is the kinetic rate constant of reactions j.

$k_{oj}$  ( $mol/kg\ cat.s$ ) is the pre-exponential factor of reactions j.

$Keq_j$  is the equilibrium constant of reaction j (j = 1, 2 and 5)

$K_i$  is the adsorption coefficient of species i (i = CH<sub>4</sub>, H<sub>2</sub>O, CO, H<sub>2</sub> and O<sub>2</sub>)

$K_i^o$  is adsorption constant of species i (i= CH<sub>4</sub> and O<sub>2</sub>) for oxidation reaction

$K_{oi}$  ( $kJ/mol$ ) is the Van't Hoff parameters of species i

$p_i$  ( $bar$ ) is the partial pressure of gas species i.

$r_j$  ( $kmol/kg\ cat.h$ ) is the rate of reactions j.

$R$  ( $kJ/kmol\ K$ ) is the universal gas constant

$T$  ( $K$ ) is the gas temperature in the reaction zone

Table 3.1 to 3.3 give the value of the Arrhenius kinetic parameters of reaction rate constants, the Van't Hoff parameters for species adsorption for the calculations of the reaction rate and the equilibrium constants of reactions.

**Table 3.1** Arrhenius kinetic parameters

reaction	parameter	$k_{oj}$	$Ea_j$
1	$k_1$	$1.17 \times 10^{15} \text{ bar}^{0.5}$	$240.10 \times 10^3$
2	$k_2$	$2.83 \times 10^{14} \text{ bar}^{0.5}$	$243.90 \times 10^3$
3	$k_3$	$5.43 \times 10^5 \text{ bar}^{-1}$	$67.13 \times 10^3$
4	$k_{4,a}$	$8.11 \times 10^5 \text{ bar}^2$	$86.00 \times 10^3$
	$k_{4,b}$	$6.82 \times 10^5 \text{ bar}^2$	$86.00 \times 10^3$

**Table 3.2** The equilibrium constant of reactions

Reaction	$K_{oj}$	$H_j$
1	$5.75 \times 10^{12}$	11476
2	$7.24 \times 10^{10}$	-4639
3	$1.26 \times 10^{-2}$	21646

**Table 3.3** Van't Hoff parameters for the expression

Adsorption coefficient	$K_{oi}$	$\Delta H_{ads,i}$
$K_{CH_4}^o$	$1.26 \times 10^{-1} \text{ bar}^{-1}$	-27.23
$K_{O_2}^o$	$7.87 \times 10^{-7} \text{ bar}^{-1}$	-92.80
$K_{CH_4}$	$6.65 \times 10^{-4} \text{ bar}^{-1}$	-38.28
$K_{CO}$	$8.23 \times 10^{-5} \text{ bar}^{-1}$	-70.65
$K_{H_2}$	$6.12 \times 10^{-9} \text{ bar}^{-1}$	-82.90
$K_{H_2O}$	$1.77 \times 10^5$	88.68

The intraparticle transport limitation is accounted by the effectiveness factor ( $\eta_j$ ) (Groote and Froment, 1996). The values of the effectiveness factors for each reaction are summarized in Table 3.4.

**Table 3.4** The effectiveness factors of reactions

Reaction	$\eta_j$
1	0.07
2	0.06
3	0.70
4	0.05

### 3.3 Membrane reactor

Membrane is a barrier that only allows certain components to pass through it. The selectivity of the membrane is controlled by its pore diameter. Membrane reactor combines reaction with separation to increase conversion, making the process more economical. Membrane reactors are most commonly used when a reaction involves some form of catalyst, and there are two main types of these membrane reactors:

- The inert membrane reactor allows catalyst pellets to flow with the reactants on the feed side (usually the inside of the membrane). It is known as an Inert Membrane Reactor with Catalyst on the Feed side. In this kind of membrane reactor, the membrane does not participate in the reaction directly; it simply acts as a barrier to the reactants and some products.
- The catalytic membrane reactor has a membrane which is coated or is made of a material that contains catalyst, which means that the membrane itself participates in the reaction. Some of the reaction products pass through the membrane and exit the reactor on the permeate side.

The main membrane functions in membrane reactors can be classified in three groups that relate to function of membrane in the process as described below.

- (a) **An extractor:** the removal of product increases the reaction conversion by shifting the reaction equilibrium. This membrane reactor has been applied in alkane dehydrogenation, steam reforming or water gas shift reaction of methane by selectively extracting the hydrogen produced.
- (b) **A distributor:** the controlled addition of reactant limits side reaction. This membrane reactor is typically adapted to consecutive parallel reaction system such as partial oxidation reforming or oxidative coupling of methane.
- (c) **An active contactor:** the controlled diffusion of reactant to the catalyst can lead to catalytic reaction zone. The membrane acts as a diffusion barrier and does not need to be perm selective but catalytically active.

### 3.3.1 H<sub>2</sub>-selective membrane

For a H<sub>2</sub> membrane reactor, the membrane is an extractor which removes product to increase the reaction conversion by shifting the reaction equilibrium. Since the autothermal reforming involves the reversible reactions consisting of steam reforming reactions which produced carbon monoxide as in Equation (3.1) and carbon dioxide as in Equation (3.2) and water gas shift reaction as in Equation (3.5), the H<sub>2</sub> perm-selectivity of membrane and its permeability have two important factors controlling the efficiency of the process. The permeability of hydrogen through the H<sub>2</sub> permeable membrane is calculated by Equation (3.13).

$$J_{H_2} = \frac{P_{m,H_2} \exp\left(-\frac{E_{A,H_2}}{RT}\right)}{\delta_{H_2}} \left(\sqrt{p_{H_2}^{high}} - \sqrt{p_{H_2}^{low}}\right) \quad (3.13)$$

The apparent activation energy  $E_{A,H_2}$  and pre-exponential factor  $P_{m,H_2}$  of the membrane are  $29.73 \text{ kJ/mol}$  and  $7.71 \times 10^{-4} \text{ mol m/(m}^2 \text{ bar}^{0.5} \text{ s)}$ , respectively (Basile et. al., 2001).  $\delta_{H_2}$  is the thickness of membrane layer (m), and  $p_{H_2}^{high}$  and  $p_{H_2}^{low}$  are the higher and lower partial pressure of H<sub>2</sub> on the two sides of the membrane, respectively.

### 3.3.2 O<sub>2</sub>-selective membrane

For this membrane reactor, the O<sub>2</sub> membrane, acted as a distributor, is used to control the supply of O<sub>2</sub> in a fixed bed of catalyst in order to control the addition of reactant to the reaction side. In autothermal reforming, air is used instead of pure O<sub>2</sub>, so the O<sub>2</sub> perm-selectivity of the membrane is an important economic factor. In general, the perovskite membrane derived from  $La_{0.2}Ba_{0.8}Fe_{0.8}Co_{0.2}O_{3-\delta}$  is used for O<sub>2</sub> permeation. The permeability of oxygen through this membrane is calculated by:

$$J_{O_2} = \frac{P_{m,O_2} \bar{T} \exp\left(-\frac{E_{A,H_2}}{RT}\right)}{\delta_{O_2}} \ln\left(\frac{p_{O_2}^{high}}{p_{O_2}^{low}}\right) \quad (3.14)$$

The apparent activation energy  $E_{A,O_2}$  and pre-exponential factor  $P_{m,O_2}$  of the membrane are  $63 \text{ kJ/mol}$  and  $7.34 \times 10^{-7} \text{ mol/(mK s)}$ , respectively (Tsai et. al., 1995 and Tsai et. al., 1997).  $\delta_{O_2}$  is the thickness of membrane layer (m) and  $p_{O_2}^{high}$  and  $p_{O_2}^{low}$  are the higher and lower partial pressure of  $O_2$  on the two sides of the membrane, respectively.  $\bar{T}$  represents the operating temperature of the membrane, which is equal to the average of the temperature at the reaction side and the permeable side.



สถาบันวิทยบริการ  
จุฬาลงกรณ์มหาวิทยาลัย



## CHAPTER IV

# MATHEMATICAL MODEL OF AUTOHERMAL REACTORS

### 4.1 Configuration of autothermal reactor

The configuration of a conventional methane autothermal reforming reactor considered in this work is schematically represented in Figure 4.1. The tubular reactor is packed with Ni-MgAl<sub>2</sub>O<sub>4</sub> catalyst (Xu and Froment, 1989). Feed stream consisting of methane, steam and air is fed into the reaction side to convert fuel into hydrogen-rich gas.

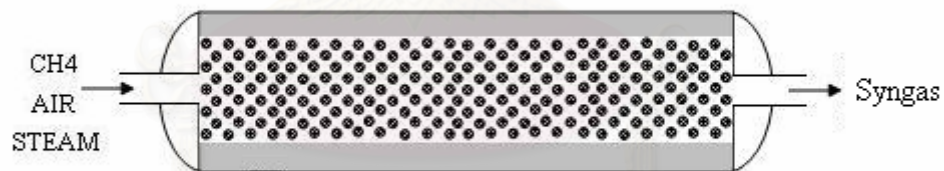


**Figure 4.1** Conventional autothermal reactor for hydrogen production

In case of an autothermal membrane reactor as shown in Figure 4.2., the inner tube of shell is coated by Pd-Ag membrane which hydrogen can permeate from the reaction side to the permeate side to form pure hydrogen stream (Figure 4.2(a)). For an autothermal O<sub>2</sub> membrane reactor, the perovskite membrane is coated on inner tube of shell. The O<sub>2</sub> from air can permeate from the non-reaction side to the reaction side to react with methane in feed stream as shown in Figure 4.2(b).

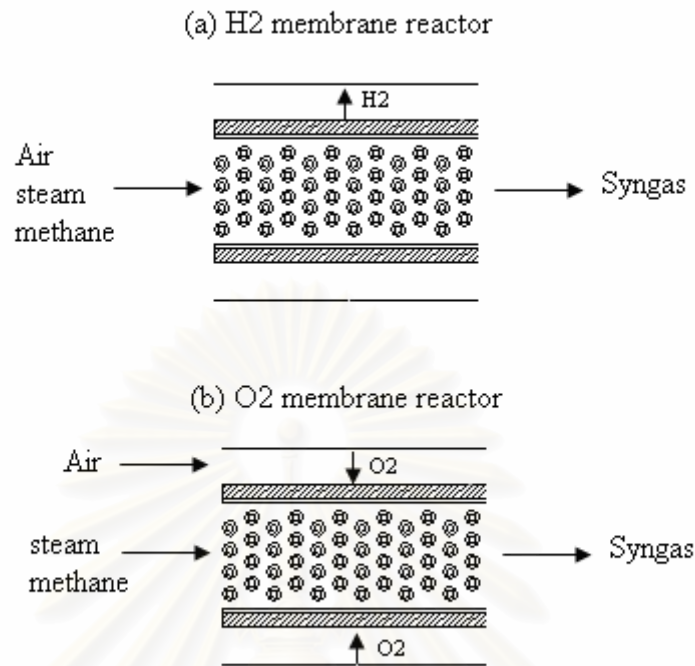


**Figure 4.2** Autothermal membrane reactors (a) H<sub>2</sub> membrane reactor (b) O<sub>2</sub> membrane reactor

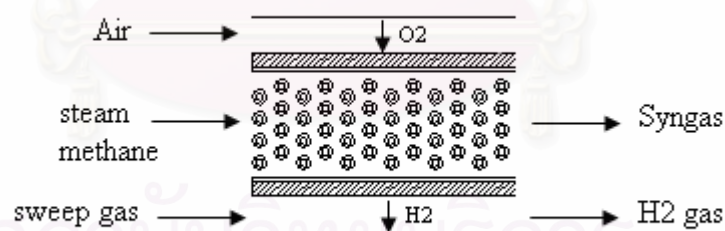


**Figure 4.3** Autothermal H<sub>2</sub>-O<sub>2</sub> membrane reactor

For an autothermal H<sub>2</sub>-O<sub>2</sub> membrane reactor, the double jacket is used. The inner tube of shell is coated with Pd-Ag membrane which separates hydrogen from the reaction side whereas the perovskite membrane is coated in another side for allowing the permeation of O<sub>2</sub> into the reaction side. The configuration of the autothermal H<sub>2</sub>-O<sub>2</sub> membrane reactor is represented in Figure 4.3.

In case study of a dual bed autothermal reactor, it is considered to be a conventional fixed-bed reactor, as schematically represented in Figure 4.4. The catalyst bed is divided into two sections. The first one is the oxidation section in which Pt-Al<sub>2</sub>O<sub>3</sub> catalyst is packed (Trimm and Lam, 1980) whereas the second one involves a steam reforming reaction and is packed with Ni-MgAl<sub>2</sub>O<sub>4</sub> catalyst (Xu and Froment, 1989). The feed consisting of methane, steam and air is introduced to the first section of reaction zone to convert fuel into hydrogen-rich gas.

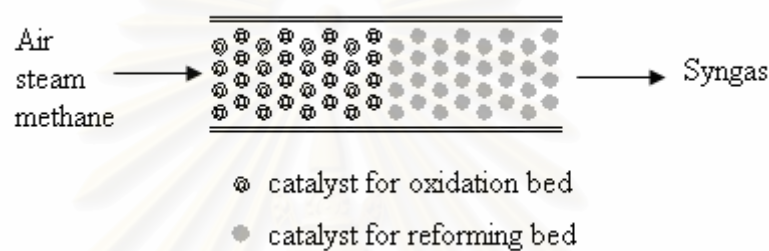


**Figure 4.4** Dual bed autothermal reforming reactor

## 4.2 Mathematic model of autothermal reactor

The reactions involving an autothermal reforming process as discussed in Chapter III are the oxidation reaction (Equation (4.1)), the steam reforming reaction which forming carbon monoxide and hydrogen (Equation (4.2)), the water gas shift reaction (Equation (4.3)) and the steam reforming reaction which forming carbon dioxide and hydrogen (Equation (4.4)):



The mathematical model of conventional and membrane autothermal reactors are based on the following basic assumptions:

- (1) one-dimensional model.
- (2) adiabatic and isobaric condition.
- (3) pseudo-homogeneous model in the catalyst bed.
- (4) ideal gas behavior.
- (5) negligible pressure drop on tube and shell sides.
- (6) no axial mixing.
- (7) only hydrogen to permeate through palladium membrane.
- (8) only oxygen gas to permeate through perovskite membrane.

#### 4.2.1 Material balance

With the assumptions specified above, the molar balance equations of component  $i$  ( $i = \text{CH}_4, \text{H}_2\text{O}, \text{O}_2, \text{CO}, \text{CO}_2$  and  $\text{H}_2$ ) for the conventional autothermal reactor can be written as follows:

$$\frac{dn_i}{dz} = \rho_{cat}(1-\varepsilon)A \sum_{j=1}^4 \eta_j r_j \quad (4.5)$$

However, for the autothermal membrane reactor, the molar balance equations are defined into the molar balances of components  $i$  at the reaction side (tube side) and the permeation side (shell side). These equations can be written as follows.

For reaction side:

$$\frac{dn_i}{dz} = \rho_{cat}(1-\varepsilon)A \sum_{j=1}^4 \eta_j r_j \pm A_m J_i \quad (4.6)$$

In case of the  $\text{O}_2$  membrane reactor,  $J_{\text{O}_2}$  as defined in Equation (3.14) is added into molar balance of oxygen specie. Similarly, for the  $\text{H}_2$  membrane reactor,

$J_{H_2}$  as defined in Equation (3.13) is applied to the mole balance equation of  $H_2$ . As  $H_2$  diffuses through the non-reaction side, the sign of  $J_{H_2}$  is negative.

For permeation side:

$$\frac{dn_i}{dz} = \pm A_m J_i \quad (4.7)$$

This equation is used for oxygen molar balance in the  $O_2$  membrane reactor, for hydrogen molar balance in the  $H_2$  membrane reactor and both species in the  $H_2$ - $O_2$  membrane reactor.

#### 4.2.2 Energy balance

Since the autothermal reactor is assumed to be operated under non-isothermal condition, the energy balance equation is involved for described the variation of reactor temperature. The energy balance of a conventional autothermal reactor at the reaction side can be written as:

$$\frac{dT}{dz} = \frac{\rho_{cat}(1-\varepsilon)A \sum_j \eta_j r_j (-\Delta H_{r,j})}{\sum_i n_i C p_i} \quad (4.8)$$

In case of an autothermal membrane reactor, the energy balance equations can be written for the reaction side (tube side) and the permeation side (shell side) as shown in Equation (4.9)-(4.12):

For the autothermal  $O_2$  membrane reactor:

$$\frac{dT_{tube}}{dz} = \frac{1}{\sum_i n_i C p_i} \left( \rho_{cat} (1 - \varepsilon) A \sum_j \eta_j r_j (-\Delta H_{r,j}) - q_{O_2} + A_{mO_2} J_{O_2} \Delta H_{O_2} \right) \quad (4.9)$$

$$\frac{dT_{shell}}{dz} = \frac{(q_{O_2} - A_{mO_2} J_{O_2} \Delta H_{O_2})}{n_{N_2} C p_{N_2} + n_{O_2} C p_{O_2}} \quad (4.10)$$

For the autothermal H<sub>2</sub> membrane reactor:

$$\frac{dT_{tube}}{dz} = \frac{1}{\sum_i n_i C p_i} \left( \rho_{cat} (1 - \varepsilon) A \sum_j \eta_j r_j (-\Delta H_{r,j}) - q_{H_2} - A_{mH_2} J_{H_2} \Delta H_{H_2} \right) \quad (4.6)$$

$$\frac{dT_{shell}}{dz} = \frac{(q_{H_2} + A_{mH_2} J_{H_2} \Delta H_{H_2})}{n_{N_2} C p_{N_2} + n_{H_2} C p_{H_2}} \quad (4.7)$$

For the autothermal H<sub>2</sub>-O<sub>2</sub> membrane reactor:

$$\frac{dT_{tube}}{dz} = \frac{1}{\sum_i n_i C p_i} \left( \rho_{cat} (1 - \varepsilon) A \sum_j \eta_j r_j (-\Delta H_{r,j}) - q_{H_2} - q_{O_2} + A_{mO_2} J_{O_2} \Delta H_{O_2} - A_{mH_2} J_{H_2} \Delta H_{H_2} \right) \quad (4.8)$$

$$\frac{dT_{shell,O_2}}{dz} = \frac{(q_{O_2} - A_m J_{O_2} \Delta H_{O_2})}{n_{N_2} C p_{N_2} + n_{O_2} C p_{O_2}} \quad (4.9)$$

$$\frac{dT_{shell,H_2}}{dz} = \frac{(q_{H_2} + A_m J_{H_2} \Delta H_{H_2})}{n_{N_2} C p_{N_2} + n_{H_2} C p_{H_2}} \quad (4.10)$$

where,  $q$  is the heat flux between the tube side and the shell side of H<sub>2</sub> membranes and O<sub>2</sub> membrane as expressed in the following equations:

$$q_{O_2} = \frac{A_{mO_2} k_{mO_2}}{x_{mO_2}} (T_{tube} - T_{shell}) \quad (4.11)$$

$$q_{H_2} = \frac{A_{mH_2} k_{mH_2}}{x_{mH_2}} (T_{shell} - T_{tube}) \quad (4.12)$$

where  $A$  is the cross section area of reactor,  $m^2$

$A_m$  is membrane area per unit length,  $m^2 / m$

$Cp_i$  is the heat capacity of component  $i$ ,  $J / mol K$

$J_i$  is the permeation flux of component  $i$  ( $i = O_2$  and  $H_2$ ),  $mol / m^2 s$

$x_m$  is the thickness of membrane tube,  $m$

$\rho_{cat}$  is the density of catalyst,  $kg / m^3$

$\varepsilon$  is the void of catalyst bed

$\Delta H_{r,j}$  is the heat of reaction  $j$ ,  $J / mol$

$\Delta H_{O_2}$  is the heat transfer by permeating  $O_2$  from air side to tube side,  $J / mol$

$\Delta H_{H_2}$  is the heat transfer by permeating  $H_2$  from tube side to  $H_2$  side,  $J / mol$

### 4.3 Reactor performance

The autothermal membrane reactors, i.e.,  $H_2$ -selective membrane reactor,  $O_2$ -selective membrane reactor and  $H_2$ - $O_2$  selective membrane reactor are investigated in this work. The effect of operating conditions, i.e., mode of operations (vacuum condition), pressure and temperature of permeation side are studied in terms of methane conversion, temperature outlet of gas,  $H_2$  recovery yield and separation factor.

The hydrogen recovery yield of the two autothermal membrane reactors, i.e., the  $H_2$ -selective membrane reactor and  $H_2$ - $O_2$  selective membrane reactor, can be computed from the amount of hydrogen produced and the amount of methane consumed to the reactor as shown in Equation (4.13):

$$Y_{H_2, recovery} = \frac{\text{mole } H_2 \text{ produced}}{\text{mole } CH_4 \text{ consumed}} \quad (4.13)$$

The separation factor of hydrogen ( $\alpha_{H_2}$ ) is determined from Equations (4.14) for the autothermal membrane reactor used the H<sub>2</sub>-selective membrane in the reactor. This parameter indicates the separation of hydrogen from synthesis gas to produce pure hydrogen gas.

$$\alpha_{H_2} = \frac{\text{mole } H_{2,\text{permeated}}}{\text{mole } H_{2,\text{effluented}} + \text{mole } H_{2,\text{permeated}}} \quad (4.14)$$



สถาบันวิทยบริการ  
จุฬาลงกรณ์มหาวิทยาลัย



# CHAPTER V

## SIMULATION RESULTS AND DISCUSSION

In this chapter, the simulation results of a methane autothermal reforming reactor for hydrogen production are presented. Three different reactors, i.e., a conventional reactor, a dual bed reactor, and a membrane reactor are considered. For the membrane reactor, three types of membrane, i.e., H<sub>2</sub>-selective membrane, O<sub>2</sub>-selective membrane, and H<sub>2</sub>-O<sub>2</sub> selective membrane, are applied to. The influences of operating parameters such as mode of operations (vacuum condition), pressure and temperature of permeation side, on the performance of these reactors in terms of methane conversion, temperature outlet of gas, H<sub>2</sub> recovery yield, and separation factor under steady state and non-isothermal conditions are analyzed.

### 5.1 Model validation

The validation of the autothermal reforming reactor model presented in Chapter IV is performed by comparing the result of model prediction in case of a conventional autothermal reactor fed by methane with industrial data published in literature (Groote, and Froment, 1996). Table 5.1 shows a comparison of simulation results and industrial data. It can be seen that the model prediction agrees very well with the industrial data.

### 5.2 Simulation results of a conventional autothermal reactor

In this section, simulation results of the conventional autothermal reactor for hydrogen production from methane are presented. As earlier mentioned, the reactor considered is an adiabatic fixed-bed reactor in which Ni-MgAl<sub>2</sub>O<sub>4</sub> catalysts are packed (Xu and Froment, 1989). The feed stream consisting of methane, steam and

air, are introduced to the reactor to carry out reforming reactions of methane as a fuel to produce hydrogen-rich gas.

**Table 5.1** Comparison of simulation results of a conventional autothermal reactor with industrial data (Groote and Froment, 1996)

Conditions	Industrial	Simulation
$F_{CH_4}$ (mol/s)	40.24	40.24
$O_2/CH_4$	0.598	0.598
$H_2O/CH_4$	1.40	1.40
$P_T$ (bar)	25.33	25.33
$T_{in}$ (K)	808	808
$T_{outlet}$ (K)	1223	1225
Product yield (mol fraction)		
$y_{CH_4}$	0.008	0.001
$y_{H_2O}$	0.306	0.303
$y_{O_2}$	0.000	0.000
$y_{CO}$	0.160	0.167
$y_{CO_2}$	0.070	0.070
$y_{H_2}$	0.456	0.469

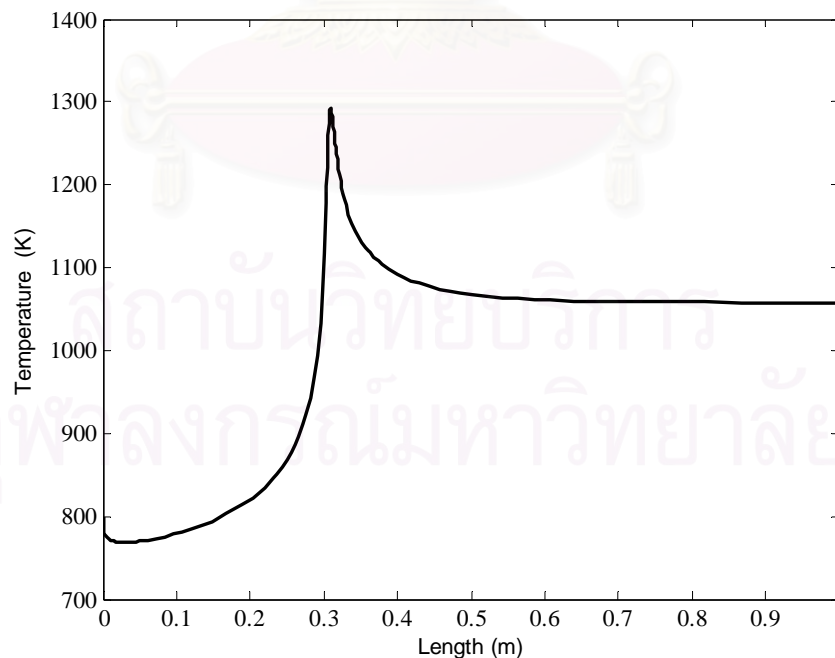
The value of the parameters for the conventional reactor is listed in Table 5.2. At the standard condition, the steam-to-fuel ratio ( $H_2O/CH_4$ ) of 1.5 and the air-to-fuel ratio ( $O_2/CH_4$ ) of 0.5 are considered.

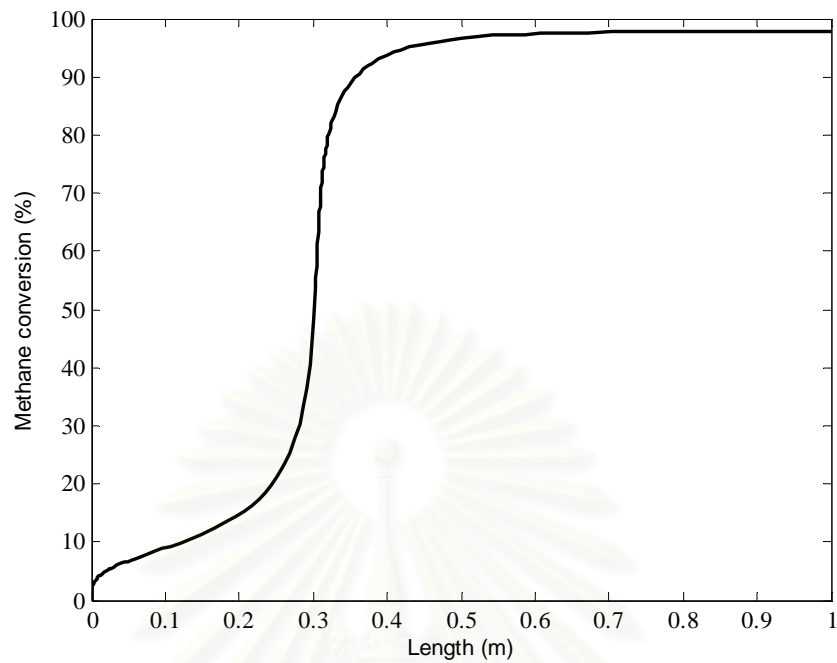
Figure 5.1 shows the temperature profile of a conventional autothermal reactor. It can be seen that the reactor temperature initially increases to the maximum temperature of 1290 K due to higher rate of exothermic oxidation reactor, compared with endothermic steam reforming reactions. Then, the temperature decreases along the length of the reactor and reaches a constant value at 1057 K. This can be explained by an increase in the methane reforming reaction.

**Table 5.2** Parameters of a conventional autothermal reactor

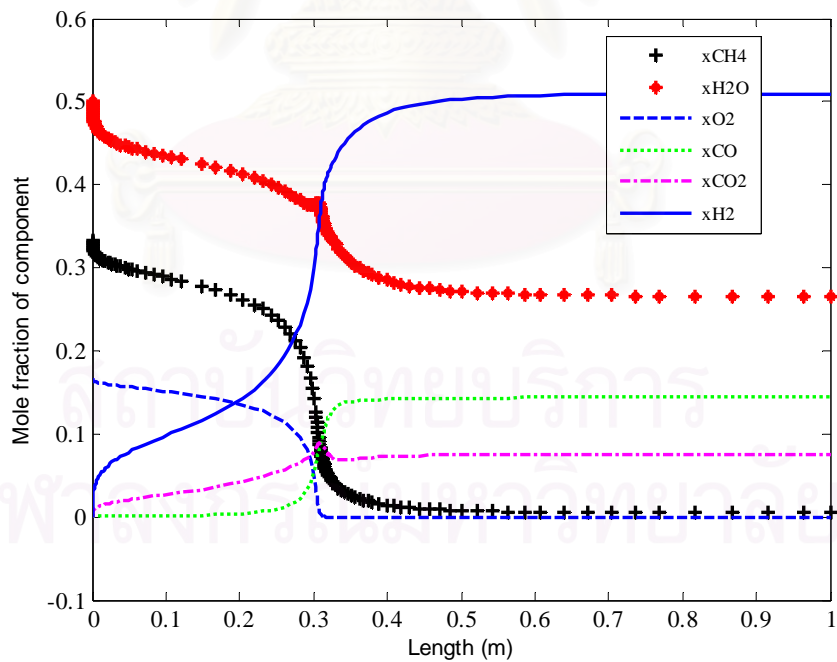
Parameters	Values	Unit
Tube radius, $r_1$	0.02	$m$
Reactor length, $L$	1	$m$
Void fraction of packing, $\varepsilon_b$	0.43	–
Catalyst density, $\rho_{cat}$	2100	$kg / m^3$
Pressure, $P_T$	14	$bar$
Temperature, $T_{in}$	800	$K$

Figure 5.2 shows a profile of a methane conversion as a function of the reactor length. The result shows that by using the conventional reformer, the methane conversion at the exit of reactor is 97.81%. The composition profile of each component in the reactor is shown in Figure 5.3. It is observed that as methane is almost completely consumed at  $z > 0.3$  m, hydrogen is less produced and no significant change in methane conversion is found.

**Figure 5.1** The temperature profile of a conventional autothermal reactor



**Figure 5.2** The methane conversion profile of a conventional autothermal reactor



**Figure 5.3** The composition profile of components in a conventional autothermal reactor

### 5.2.1 Effect of H<sub>2</sub>O/CH<sub>4</sub> ratio

In this section, the effect of H<sub>2</sub>O/CH<sub>4</sub> ratio, which is varied from 1.0-3.5, on the reactor performance in terms methane conversion, temperature outlet and hydrogen-to-carbon monoxide ratio (H<sub>2</sub>/CO) of product is given. The O<sub>2</sub>/CH<sub>4</sub> ratio of feed is fixed at 0.5. This simulation results are shown in Table 5.3. It is found that increasing the H<sub>2</sub>O/CH<sub>4</sub> ratios leads to an increase in the reaction rate of the steam reforming and water gas shift. As these reactions require energy to proceed such the reactions, the outlet reactor temperature decreases. In addition, the increased steam reforming and water gas shift reactions results in high H<sub>2</sub>/CO ratio of product.

The maximum methane conversion of 97.81% and H<sub>2</sub>/CO ratio of product of 5.96 are obtained at the H<sub>2</sub>O/CH<sub>4</sub> ratio of 1.5 and 3.5, respectively. Figures 5.4-5.5 show the profile of temperature and methane conversion at different H<sub>2</sub>O/CH<sub>4</sub> ratio. The figure shows that at higher H<sub>2</sub>O/CH<sub>4</sub> ratio, the maximum temperature within the reactor is decreased. More steam in the system increases the steam reforming reaction leading to a decreased temperature.

**Table 5.3** The effect of H<sub>2</sub>O/CH<sub>4</sub> on reactor performance at O<sub>2</sub>/CH<sub>4</sub> of 0.5

H <sub>2</sub> O/CH <sub>4</sub>	CH <sub>4</sub> conversion (%)	Temperature outlet (K)	H <sub>2</sub> /CO ratio
1.0	97.77	1067	3.00
1.5	97.81	1058	3.54
2.0	97.76	1049	4.13
2.5	97.42	1041	4.74
3.0	96.38	1037	5.37
3.5	93.77	1042	5.96

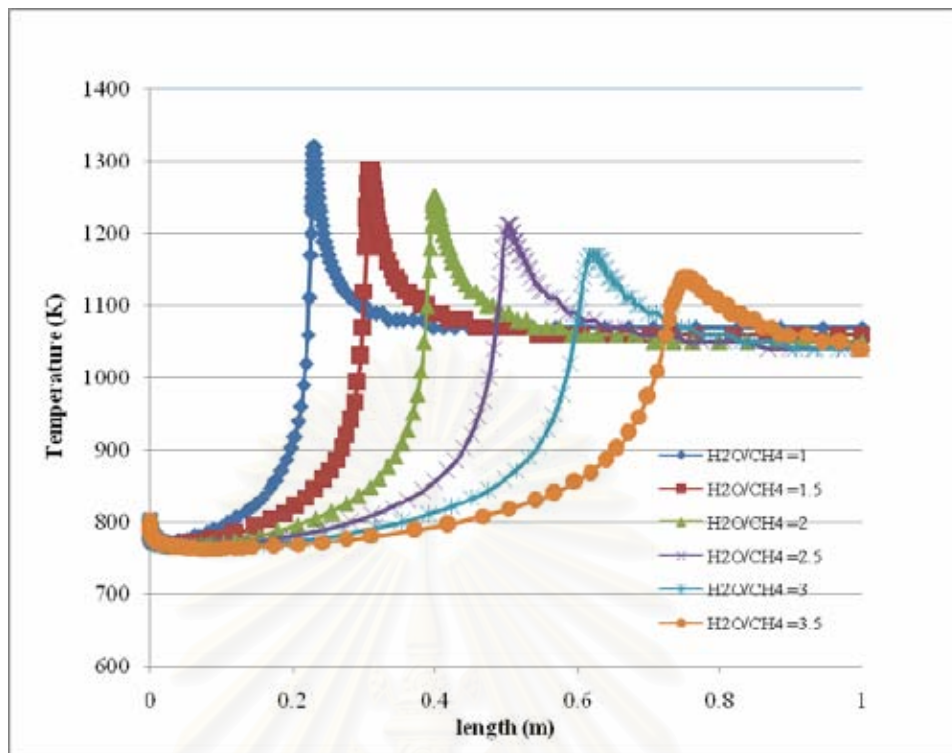


**Figure 5.4** Temperature profile of a conventional reactor by varying  $\text{H}_2\text{O}/\text{CH}_4$  ratio

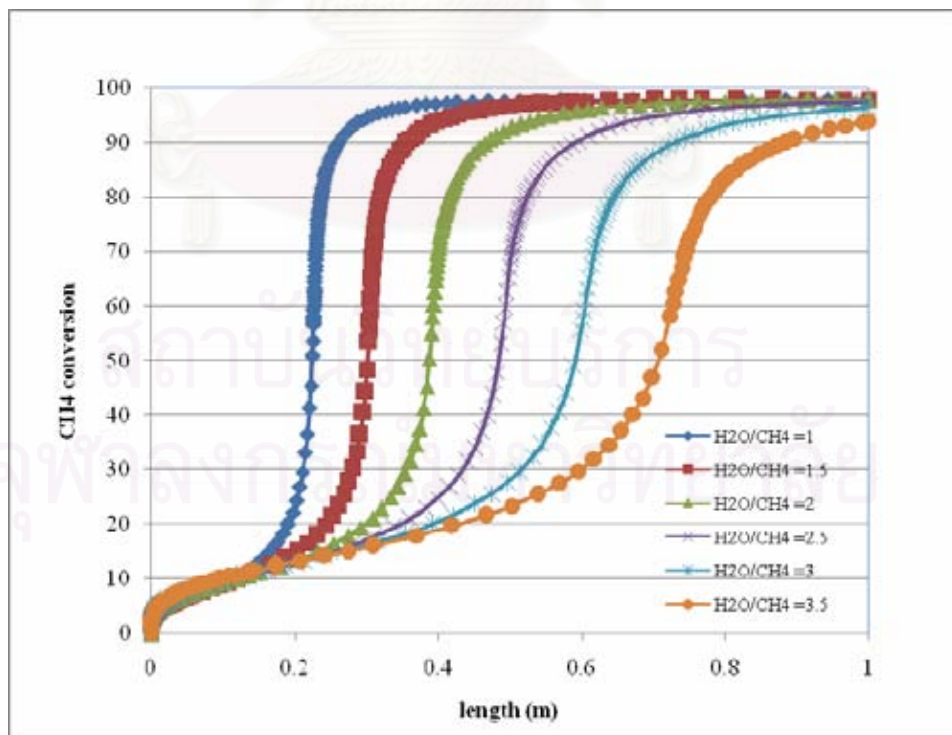


**Figure 5.5** Methane conversion profile of conventional reactor by varying  $\text{H}_2\text{O}/\text{CH}_4$  ratio

### 5.2.2 Effect of O<sub>2</sub>/CH<sub>4</sub> ratio

Table 5.4 shows the effect of O<sub>2</sub>/CH<sub>4</sub> ratio on the reactor performance when the H<sub>2</sub>O/CH<sub>4</sub> ratio is fixed at 1.5. The simulation results show that the products obtained have the H<sub>2</sub>/CO ratio in the range of 2.89 – 5.65. The feed with higher O<sub>2</sub>/CH<sub>4</sub> ratio can increase the oxidation rate because oxygen has more active with methane than others so high maximum temperature is observed (Figure 5.6). This leads to low H<sub>2</sub> and CO. However, an increase in the O<sub>2</sub>/CH<sub>4</sub> ratio results in an increase of the methane conversion as a result of high oxidation and reforming. Figure 5.7 shows the methane conversion profile along the length of the reactor.

**Table 5.4** The effect of O<sub>2</sub>/CH<sub>4</sub> on reactor performance at H<sub>2</sub>O/CH<sub>4</sub> ratio of 1.5

O <sub>2</sub> /CH <sub>4</sub>	CH <sub>4</sub> conversion (%)	Temperature outlet (K)	H <sub>2</sub> /CO ratio
0.30	66.73	927	5.65
0.35	76.29	948	4.91
0.40	85.14	973	4.37
0.45	92.74	1006	3.93
0.50	97.81	1058	3.54
0.55	99.59	1132	3.19
0.60	99.92	1214	2.89

สถาบันวิทยบริการ  
จุฬาลงกรณ์มหาวิทยาลัย

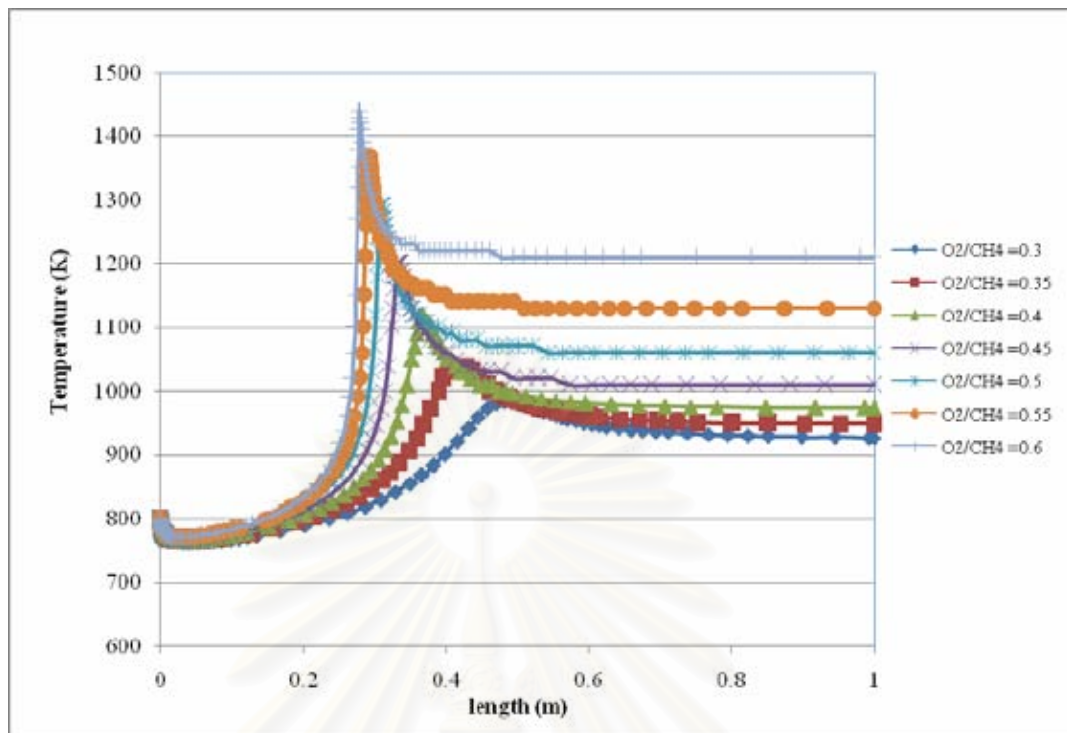


Figure 5.6 Temperature profile of a conventional reactor by varying  $O_2/CH_4$  ratio

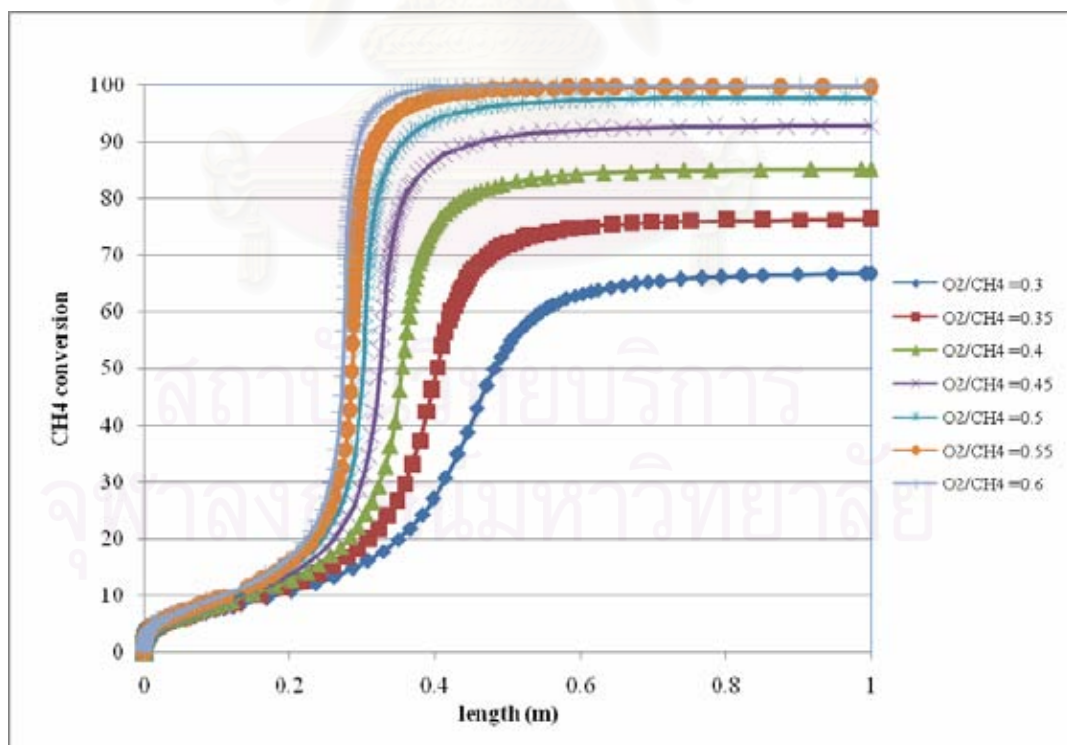


Figure 5.7 Methane conversion profile of a conventional reactor by varying  $O_2/CH_4$  ratio



### 5.2.3 Effect of feed position of steam

Since the autothermal reforming reactions involve steam, carbon dioxide, carbon monoxide and hydrogen, steam fed with methane and oxygen would have a significant effect on hydrogen production. From the previous section, it is found that adding more steam to the feed reduces the maximum reactor temperature which in turn leads to lower reforming and combustion rates. In addition, the equilibrium of the water gas shift reaction moves towards the product side resulting in higher H<sub>2</sub>/CO product ratio. As a result, the addition of steam with fuel has key effect on the reforming rates and also the temperature in the autothermal reactor (Groote and Froment, 1996).

In this section, the impact of the addition of steam with fuel at different position of the reactor is investigated. Table 5.5 shows the simulation results of adding steam (T = 600 K) at different positions of the conventional autothermal reactor.

**Table 5.5** Simulation results of adding steam at different location of the conventional reactor

z (m)	CH <sub>4</sub> conversion (%)	Temperature outlet (K)	H <sub>2</sub> /CO ratio
0.00	97.81	1057	3.54
0.05	97.82	1033	5.94
0.10	98.36	1040	6.04
0.15	99.90	1158	5.37
0.20	99.85	1137	5.77
0.25	99.85	1133	5.77
0.30	99.85	1131	5.77

It is seen that hydrogen yield is increased when feeding steam at the position far away from the inlet. As no steam is introduced at the inlet, methane is reacted with oxygen via oxidation reactions. When steam is introduced to the reactor, methane is

also consumed from steam reforming reaction. This leads to high methane conversion and  $H_2/CO$  ratio of product. However, adding steam at the reactor position of more than 0.10 m. from the inlet, the methane conversion and  $H_2/CO$  ratio of product slightly decrease. This may be caused by the fact that the temperature of feed is reduced and thus, the rate of reforming reaction is decreased. It is also noticed that adding steam at the reactor position of more than 0.2 m. has no significant effect on  $H_2/CO$  ratio, methane conversion and outlet reactor temperature of product.

### 5.3 Simulation results of a dual bed autothermal reactor

An autothermal reforming reactor is generally an adiabatic fixed-bed reactor in the presence of mixture of two different catalysts for partial oxidation and steam reforming reactions. In this section, the performance of a methane autothermal reforming reactor in which the catalyst bed is divided into two zones; the first zone involves the partial oxidation while the second zone involves the steam reforming for improve the performance of reactor, is investigated. A gas mixture of methane, steam and air is fed into the first zone of the reactor where partial oxidation reaction is occurred to convert fuel into synthesis gas. Then the synthesis gas from the first zone enters the second zone where the steam reforming is carried out to produce hydrogen-rich-gas. It is assumed that the partial oxidation section occupy the reactor volume of 10%.

Figure 5.8 shows a comparison of the temperature distribution between the conventional and the dual bed autothermal reactors. The maximum temperature of the dual bed reactor is higher than that of the conventional reactor. It is obvious that the reactor temperature increase sharply at the first section of the dual bed reactor as a result of the oxidation reaction. The higher temperature leads to an increase in the conversion of methane as can be seen in Figure 5.9

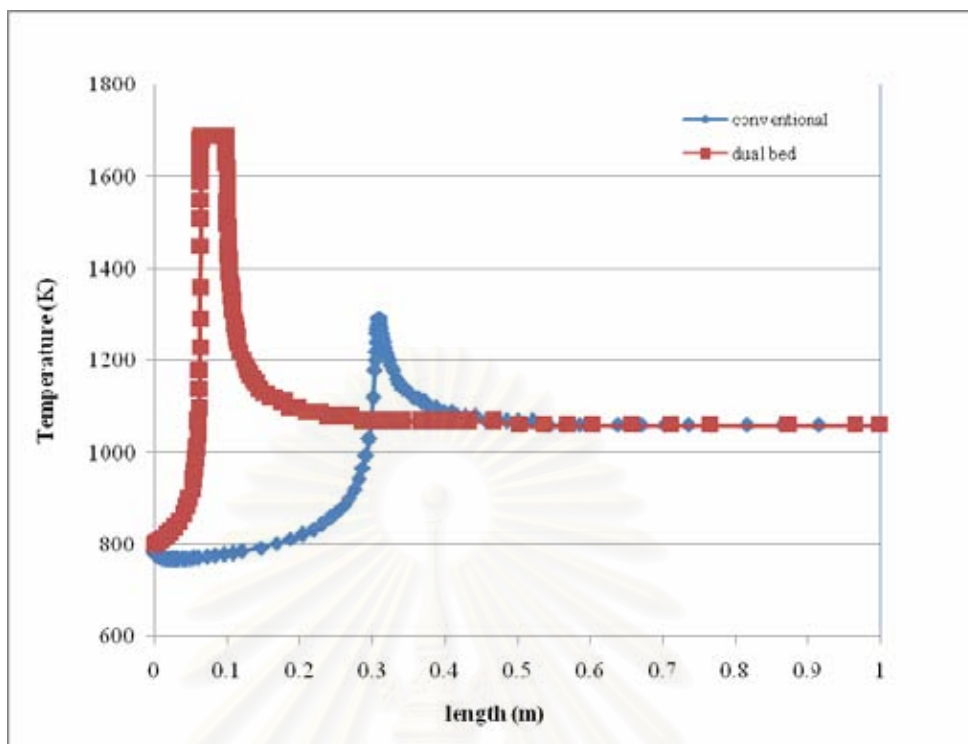


Figure 5.8 Temperature profile of a conventional and dual bed reactor

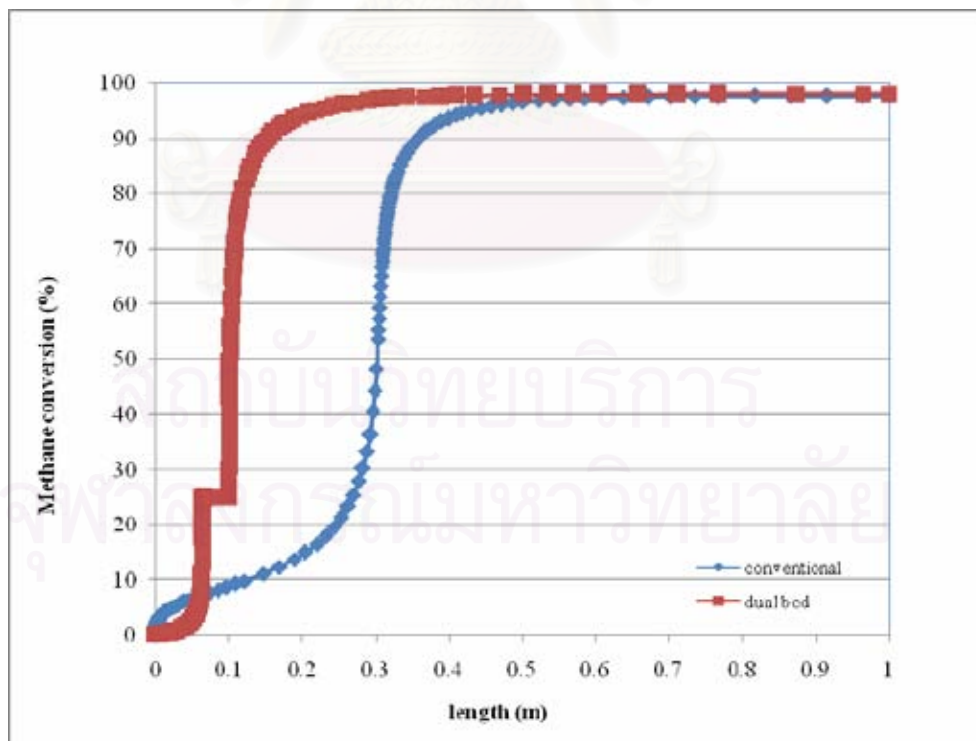


Figure 5.9 Methane conversion profile of a conventional and dual bed reactor

### 5.3.1 Effect of H<sub>2</sub>O/CH<sub>4</sub> ratio

The simulation results of the dual bed autothermal reactor with the variation of the H<sub>2</sub>O/CH<sub>4</sub> ratio are compared with the conventional autothermal reactor as shown in Table 5.6. The results indicate that at H<sub>2</sub>O/CH<sub>4</sub> ratio of 1.0-2.5, the dual bed reactor show better performance in terms of the methane conversion than the conventional reactor. Since the heat generated from oxidation reaction at the first section of the dual bed reactor is employed to preheat a synthesis gas entering the second zone, the steam reforming is more pronounced.

**Table 5.6** Comparison of the simulation results between conventional and dual bed autothermal reactors in case of varying the H<sub>2</sub>O/CH<sub>4</sub> ratio

H <sub>2</sub> O/CH <sub>4</sub>	Conventional reactor			Dual bed reactor		
	T <sub>out</sub> (K)	CH <sub>4</sub> conversion	H <sub>2</sub> /CO	T <sub>out</sub> (K)	CH <sub>4</sub> conversion	H <sub>2</sub> /CO
1.0	1067	97.77	3.00	1072	98.01	2.98
1.5	1058	97.84	3.54	1063	98.05	3.51
2.0	1048	97.75	4.13	1054	98.09	4.08
2.5	1041	97.42	4.74	1044	98.06	4.69
3.0	1037	96.38	5.37	802	35.00	10
3.5	1042	93.77	5.96	770	26.53	10
4.0	1066	87.19	6.38	758	23.79	10

As a result, the methane conversion of the dual bed reactor is higher than the conventional reactor. However, the H<sub>2</sub>/CO ratio of product from the dual bed reactor is lower than that of the conventional reactor since most oxygen is completely consumed in the first section of the dual bed reactor. By considering for the case of the H<sub>2</sub>O/CH<sub>4</sub> ratio of more than 2.5, the methane conversion and the temperature outlet of the conventional and dual bed reactors decrease with increasing H<sub>2</sub>O/CH<sub>4</sub> ratio because high amount of steam in feed lowers the oxidation and reforming rate. It is obvious that the methane conversion of the dual bed reactor dropped very fast with increasing H<sub>2</sub>O/CH<sub>4</sub> ratio from 2.5 to 4.0.

### 5.3.2 Effect of O<sub>2</sub>/CH<sub>4</sub> ratio

Oxygen may have a favorable effect on the performance of autothermal reactors since it involves the oxidation reaction. Thus, the effect of the O<sub>2</sub>/CH<sub>4</sub> ratio of feed is studied in this section. Table 5.7 shows the performance of the conventional and the dual bed autothermal reactor in terms of the methane conversion and the reactor outlet temperature. It can be seen that the H<sub>2</sub>/CO ratio of product decreases with increasing O<sub>2</sub>/CH<sub>4</sub> ratio. More oxygen in feed stream reduced the amount of methane entering the second part of the reactor, thus decreasing the steam reforming reactions and reducing the hydrogen production.

**Table 5.7** Comparison of the simulation results between conventional and dual bed autothermal reactors in case of varying O<sub>2</sub>/CH<sub>4</sub> ratio

O <sub>2</sub> /CH <sub>4</sub>	Conventional reactor			Dual bed reactor		
	T <sub>out</sub> (K)	CH <sub>4</sub> conversion	H <sub>2</sub> /CO	T <sub>out</sub> (K)	CH <sub>4</sub> conversion	H <sub>2</sub> /CO
0.30	927	66.73	5.65	928	67.54	5.57
0.35	949	76.29	4.90	950	76.99	4.85
0.40	974	85.14	4.36	975	85.77	4.32
0.45	1010	92.74	3.93	1010	93.24	3.89
0.50	1060	97.81	3.54	1063	98.07	3.51
0.55	1130	99.60	3.19	1140	99.65	3.16
0.60	1210	99.92	2.89	1222	99.93	2.87

## 5.4 Simulation results of an autothermal membrane reactor

In this section, an autothermal membrane reactor with different types of membrane is studied for the production of hydrogen from methane. The palladium-silver (Pd-Ag) membrane is applied to the reactor as a H<sub>2</sub>-selective membrane for pure hydrogen production. The perovskite ( $La_{0.2}Ba_{0.8}Fe_{0.8}Co_{0.2}O_{3-\delta}$ ) membrane is used as an O<sub>2</sub>-selective membrane for oxygen permeation. Based on such the membrane, three types of the membrane reactor are studied: a H<sub>2</sub>-selective membrane reactor, an O<sub>2</sub>-selective membrane, and a H<sub>2</sub> and O<sub>2</sub> selective membrane reactor. The effects of operation mode at the permeation side using a vacuum pump and sweep gas are investigated for the H<sub>2</sub>-selective membrane reactor. For the O<sub>2</sub>-selective membrane reactor, the effects of membrane thickness and the ratio of H<sub>2</sub>O/CH<sub>4</sub> and O<sub>2</sub>/CH<sub>4</sub> in feed stream are considered. For the H<sub>2</sub>- O<sub>2</sub> selective membrane, the effects of pressure, temperature, the amount of oxygen in air side are investigated, respectively.

### 5.4.1 H<sub>2</sub>-selective membrane reactor

The H<sub>2</sub>-selective autothermal membrane reactor consists of two concentric tubes. An internal tube is coated with Pd-Ag membrane to allow hydrogen to permeate from the reaction side to the permeate side. Table 5.8 shows the specification of the membrane reactor used in this study. For the standard conditions, the H<sub>2</sub>O/CH<sub>4</sub> ratio of 1.5 and the O<sub>2</sub>/CH<sub>4</sub> ratio of 0.5 are fixed.

**Table 5.8** Parameters of H<sub>2</sub>-selective autothermal membrane reactor

Parameters	Symbol	Values	Unit
Membrane thickness	$M_{H_2}$	10	$\mu m$
Thickness of membrane tube	$x_{mH_2}$	5	$mm$
Thermal conductivity	$k_{mH_2}$	0.15	$W / m K$
Temperature of sweep gas	$T_{sin}$	800	$K$
Pressure in permeation side	$P_S$	14	$bar$

Figures 5.10-5.12 demonstrate the profile of temperature, methane conversion, and composition within the reactor at the standard condition, respectively. It can be seen that the temperature profile of the membrane reactor is similar to the conventional autothermal reactor; however, the maximum temperature of the membrane reactor is lower. As hydrogen permeates from the reaction side to the permeation side, some heat is removed from the reaction. From Figure 5.11, methane is completely consumed at the reactor length of 0.7 m; the conversion of methane in the membrane reactor is enhanced, compared with the conventional fixed bed reactor; the reaction equilibrium is shifted to the product side due to the removal of hydrogen via membrane. The results in Figure 5.12 indicate that the mole fraction of hydrogen initially increases to its maximum of 0.4 at the reactor length of 0.4 m and then it decreases continuously to the end of reactor. The decreased hydrogen is caused by an increase in the permeation of hydrogen through the membrane.

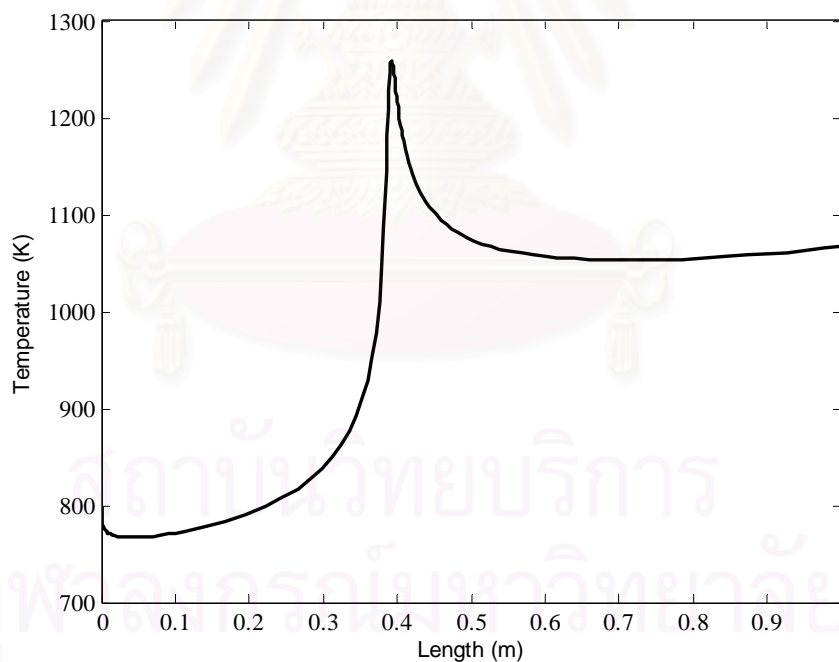


**Figure 5.10** Temperature profile of a  $H_2$ -selective membrane reactor

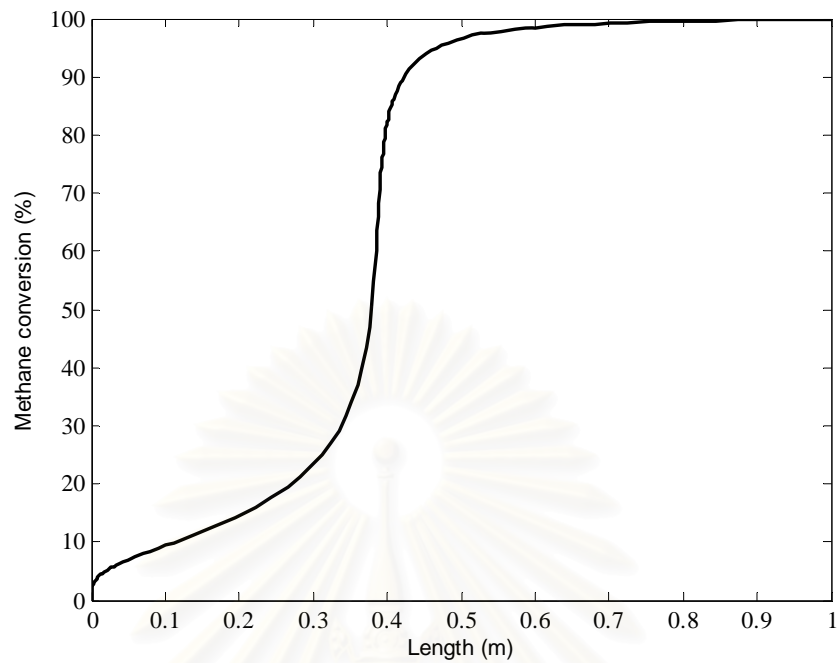


**Figure 5.11** Methane conversion profile of a  $H_2$ -selective membrane reactor

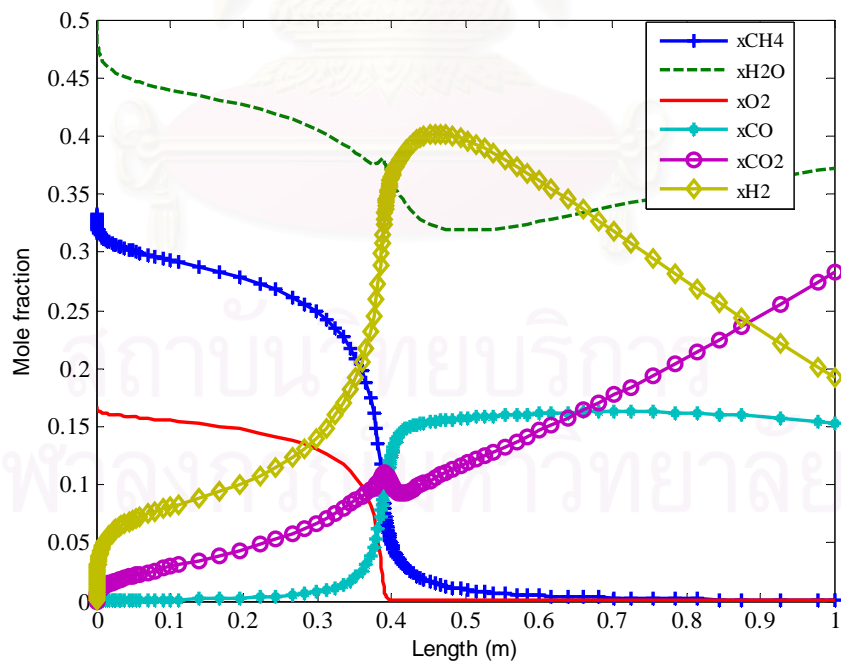


**Figure 5.12** Mole fraction profile of synthesis gas from  $H_2$ -selective membrane reactor



Figure 5.13 shows the change in the hydrogen separation factor and the yield of hydrogen. The results presents that the hydrogen separation factor initially increases along the length of reactor and slightly drops at the reactor length of 0.3-0.4 m since at the middle, the reactor is controlled by oxidation reaction and hydrogen is less produced. The maximum hydrogen separation factor  $\alpha_{H_2}$  is 0.6. Considering the hydrogen recovery yield of the H<sub>2</sub>-selective membrane reactor, it is found that it highly increases at the reactor length of 0.3-0.5 at which more hydrogen is produced from the steam reforming and water gas shift reactions. The maximum value of hydrogen yield is 2.50 mole per methane fed 1 mole.

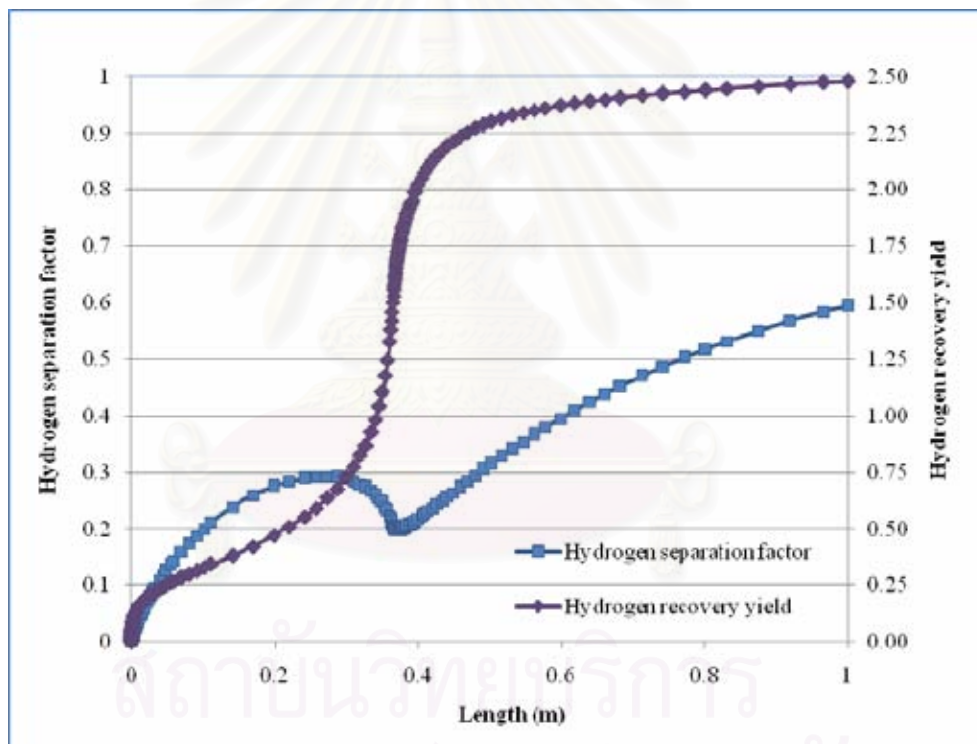


**Figure 5.13** Hydrogen separation factor and hydrogen recovery yield profile of a H<sub>2</sub>-selective membrane reactor

#### 5.4.1.1 Effect of H<sub>2</sub>O/CH<sub>4</sub> ratio

As steam involves the reforming reaction for producing hydrogen, the H<sub>2</sub>O/CH<sub>4</sub> ratio has an influence on this reactor performance. In this section, the H<sub>2</sub>O/CH<sub>4</sub> ratio is varied from 0.3-2.0 at the O<sub>2</sub>/CH<sub>4</sub> ratio of 0.5 and the reactor performance in terms of methane conversion, temperature outlet and hydrogen-to-carbon monoxide ratio (H<sub>2</sub>/CO) of product is studied. The results are demonstrated in Figures 5.14-5.15. It can be seen that the H<sub>2</sub>O/CH<sub>4</sub> ratio has a slight effect on the methane conversion and the reactor temperature.

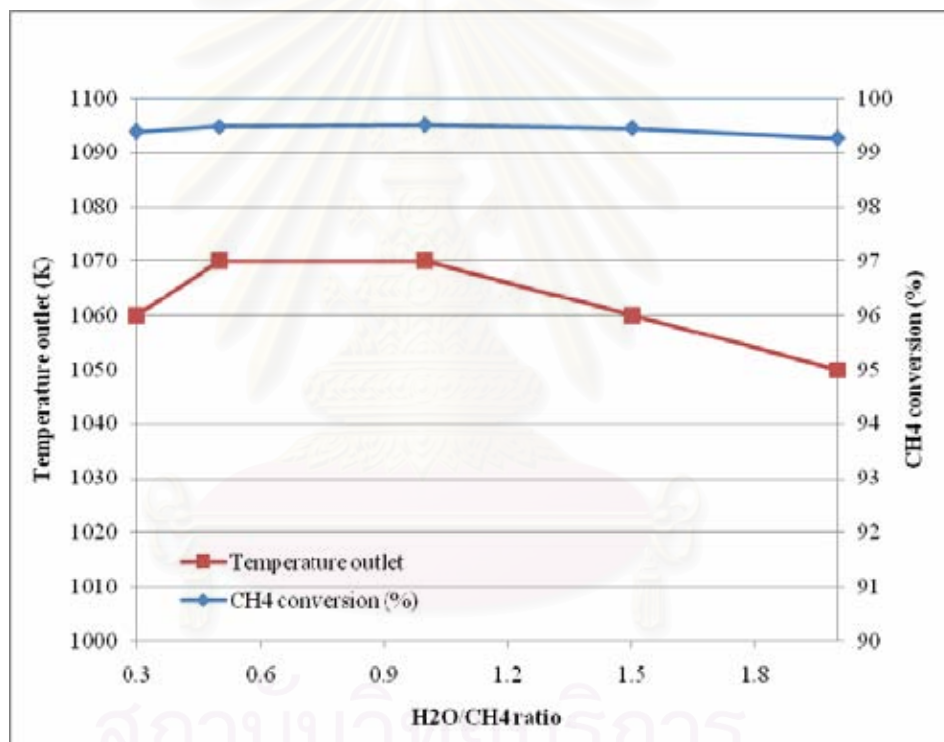


**Figure 5.14** CH<sub>4</sub> conversion and gas temperature outlet by varying H<sub>2</sub>O/CH<sub>4</sub> ratio

Considering the hydrogen separation factor, Figure 5.15 shows that it is slightly decreased with increasing the H<sub>2</sub>O/CH<sub>4</sub> ratio whereas the hydrogen recovery yield has an increased trend because of an increase in the reforming reaction. It was found that the maximum methane conversion of 99.51 can be achieved with the H<sub>2</sub>O/CH<sub>4</sub> ratio of 1.0 whereas the maximum hydrogen separation factor is 0.72 with the H<sub>2</sub>O/CH<sub>4</sub> ratio of 0.3.

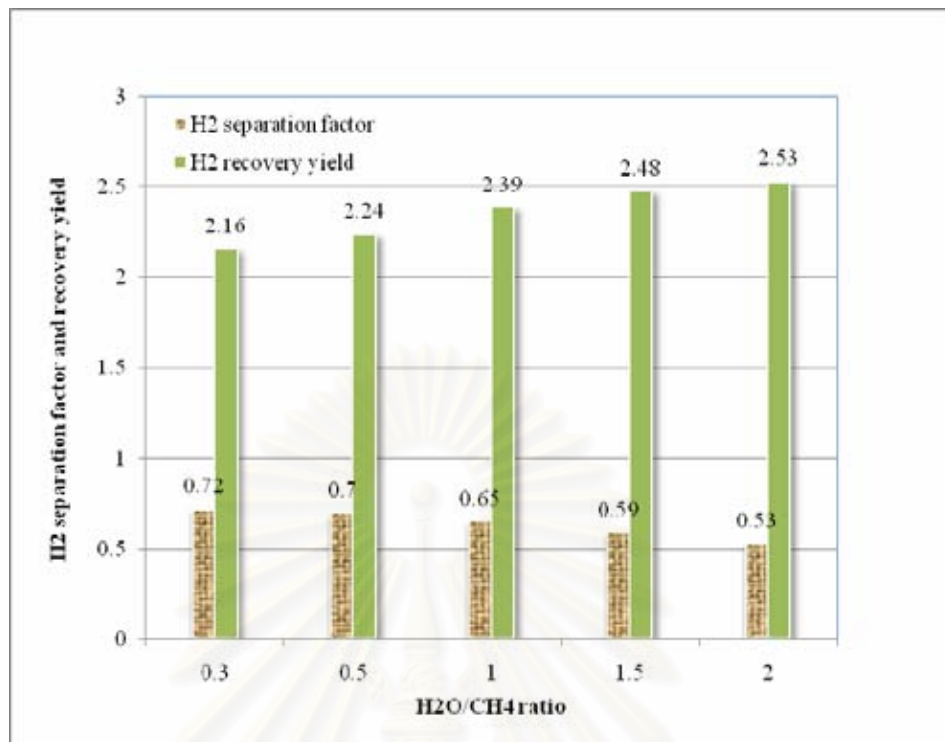


**Figure 5.15** Hydrogen separation factor and recovery yield by varying H<sub>2</sub>O/CH<sub>4</sub> ratio

#### 5.4.1.2 Effect of O<sub>2</sub>/CH<sub>4</sub> ratio

Figures 5.16-5.17 shows the result of varying the O<sub>2</sub>/CH<sub>4</sub> ratio of feed from 0.3 to 1.0. It is found that the methane conversion increases with increasing the O<sub>2</sub>/CH<sub>4</sub> ratio since oxygen can react with more methane leading to higher methane conversion. As the reactor operating temperature increases as a result of high exothermic oxidation, more hydrogen is generated from methane steam reforming. The methane conversion and gas temperature outlet resulted from varying O<sub>2</sub>/CH<sub>4</sub> ratio are in the range of 68.76-99.99% and 900-1960 K, respectively. The maximum methane conversion and gas temperature outlet are 99.99% and 1960 K at the O<sub>2</sub>/CH<sub>4</sub> ratio of 1.0.

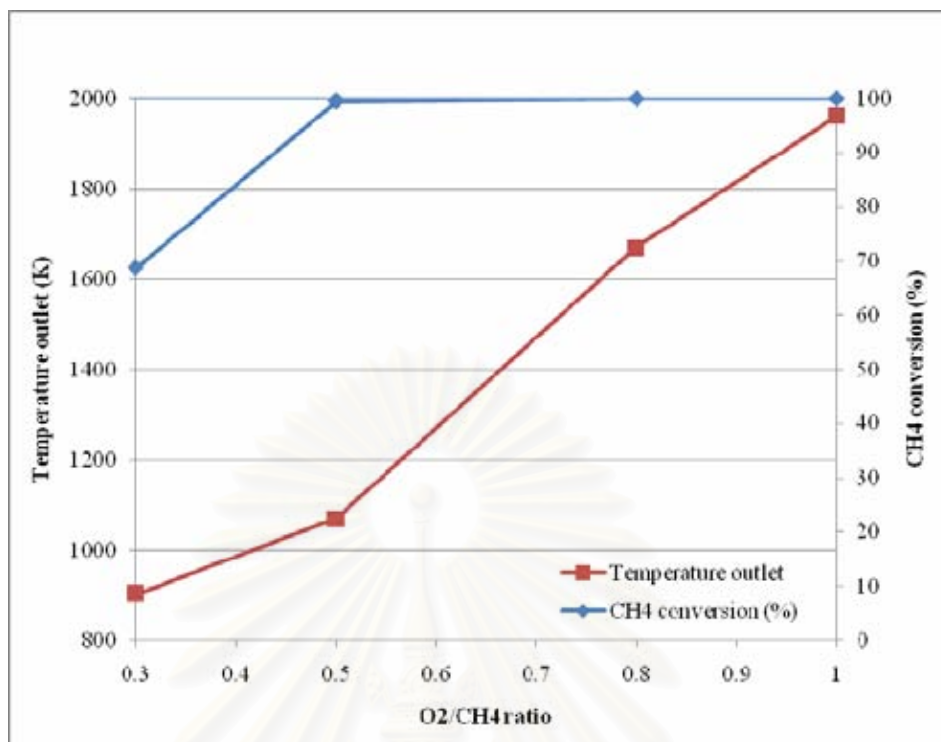


**Figure 5.16** CH<sub>4</sub> conversion and gas temperature outlet by varying O<sub>2</sub>/CH<sub>4</sub> ratio

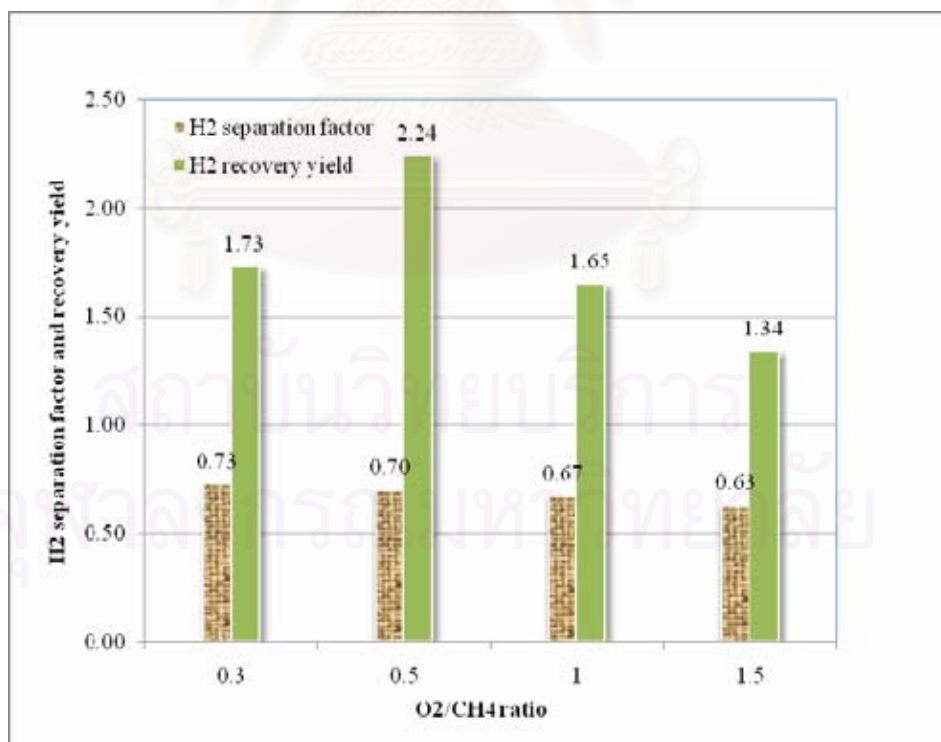


**Figure 5.17** Hydrogen separation factor and recovery yield by varying O<sub>2</sub>/CH<sub>4</sub> ratio

However, it is observed that the hydrogen recovery yield ( $Y_{H_2, recovery}$ ) decreases with increasing the  $O_2/CH_4$  ratio as shown in Figure 5.17. This can be explained that when oxygen in feed gas increases, methane is more consumed by oxidation reaction than steam reforming, thus resulting in decreased hydrogen. The result shows that the maximum yield of hydrogen ( $Y_{H_2, recovery}$ ) is 72.67% when the gas feed is with the  $O_2/CH_4$  ratio of 0.3. However, at this condition, the lowest methane conversion of 68.76% is observed because the heat supplied to the endothermic reforming reaction is reduced at the low ratio of  $O_2/CH_4$ .

#### 5.4.1.3 Effect of membrane thickness

In this section, the effect of the membrane thickness on the reactor performance in terms of the hydrogen separation factor is studied. Figure 5.18 shows that more hydrogen in the permeation side can be achieved when lower membrane thickness is used in the reactor.

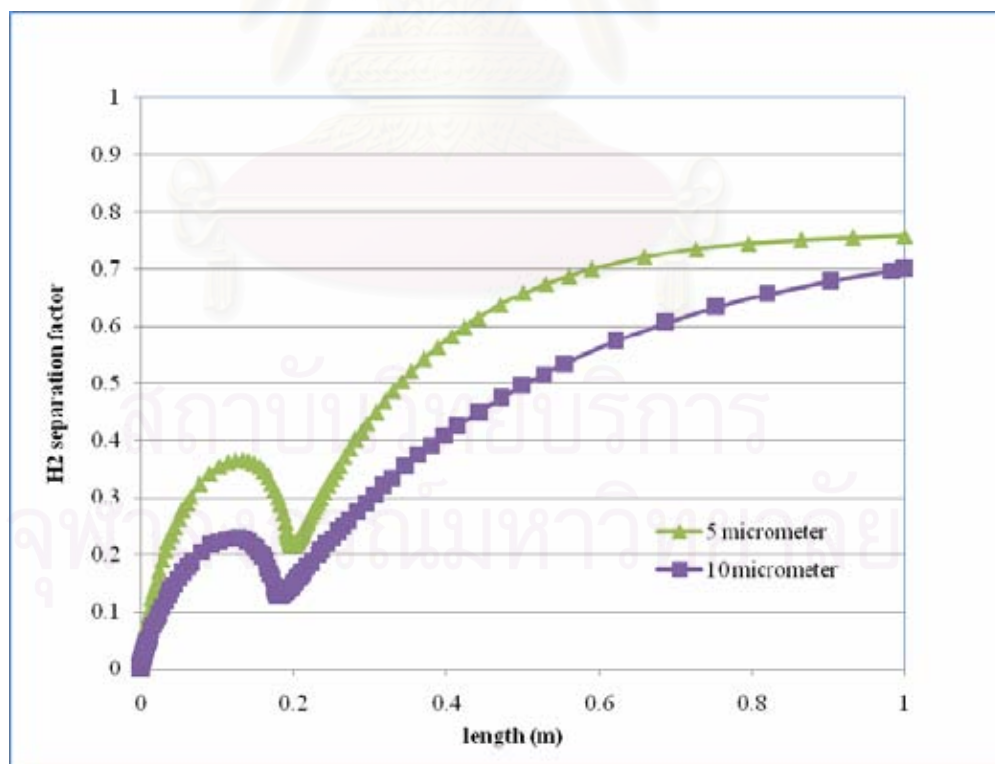


**Figure 5.18** Hydrogen separation factor by varying thickness of  $H_2$ -selective membrane

#### 5.4.1.4 Effect of operation mode

In this section, an autothermal H<sub>2</sub>-selective membrane reactor operated under a vacuum condition is considered. Vacuum pressure is used as the driving force for the permeation of hydrogen across the membrane instead of using sweep gas. It is assumed that the pressure at the shell side is 0.05 bars. Figures 5.19-5.20 illustrates the profile of gas composition, hydrogen separation factor ( $\alpha_{H_2}$ ) and the hydrogen recovery yield ( $Y_{H_2, recovery}$ ). It can be seen that more hydrogen can permeate through the membrane, thus increasing the water shift reaction rate; higher CO<sub>2</sub> is observed.

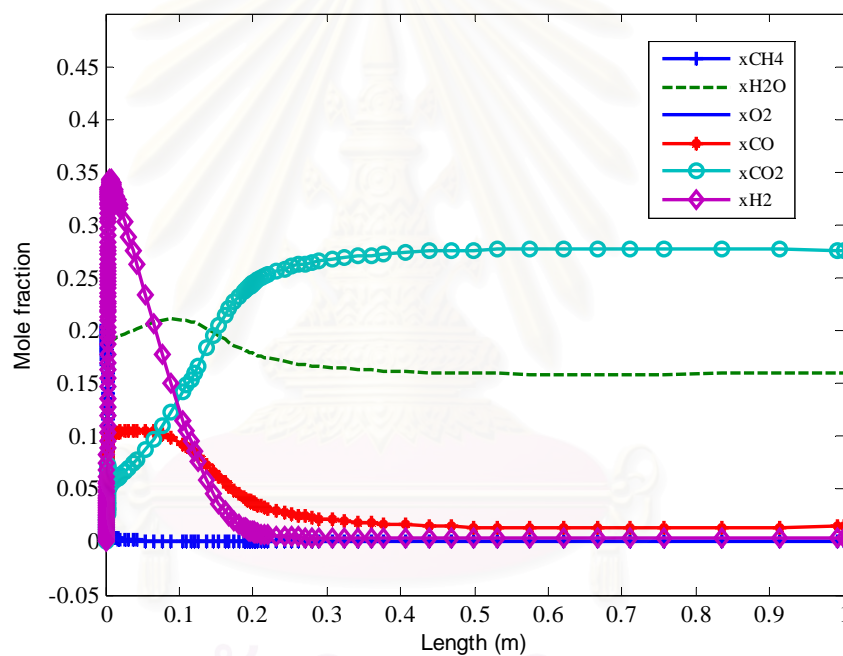


**Figure 5.19** Composition profile of synthesis gas from H<sub>2</sub>-selective membrane reactor (under vacuum operation)

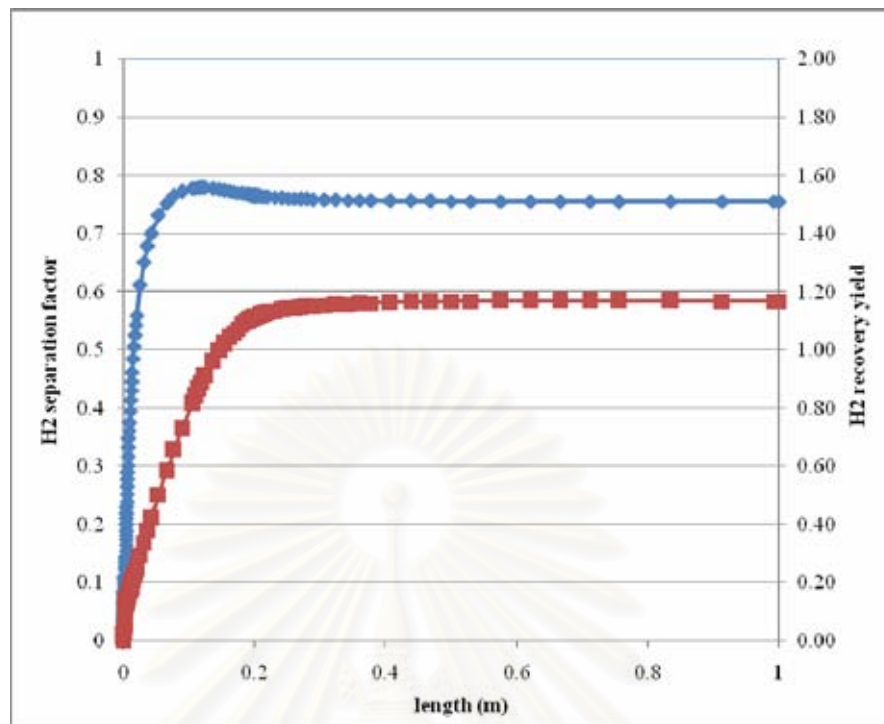


**Figure 5.20** H<sub>2</sub> separation factor and recovery yield of H<sub>2</sub>-selective membrane reactor (vacuum condition)

#### 5.4.2 O<sub>2</sub>-selective membrane reactor

Oxidation reaction has a key effect on the peak of the reactor temperature which may deteriorate the activity of catalyst. In this section, an autothermal O<sub>2</sub>-selective membrane reactor is applied to produce hydrogen from methane; O<sub>2</sub>-selective membrane derived from perovskite membrane is used to control oxygen entering the reaction side. The reactor parameters are listed in table 5.9.

**Table 5.9** Parameters of O<sub>2</sub>-selective autothermal membrane reactor

Parameters	Symbol	Values	Unit
Membrane thickness	$M_{O_2}$	5	$\mu m$
Thickness of membrane tube	$x_{mO_2}$	5	$mm$
Thermal conductivity	$k_{mO_2}$	0.30	$W / m K$
Temperature of sweep gas	$T_{sin}$	800	$K$
Pressure in shell side	$P_S$	14	$bar$

It is assumed that the inlet gas with the  $\text{H}_2\text{O}/\text{CH}_4$  ratio of 1.0 and  $\text{O}_2/\text{CH}_4$  ratio of 0.5 is fed to the autothermal  $\text{O}_2$ -selective membrane reactor. Figures 5.21-5.22 shows the temperature and methane conversion profiles along the length of the reactor. The reactor temperature steadily increases from the inlet.

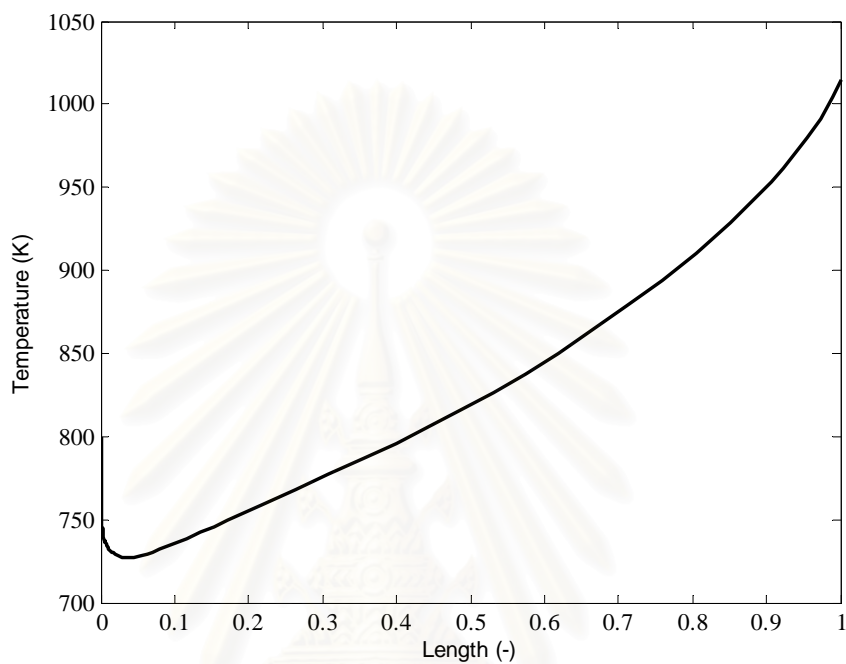


**Figure 5.21** Temperature profile of an  $\text{O}_2$ -selective membrane reactor

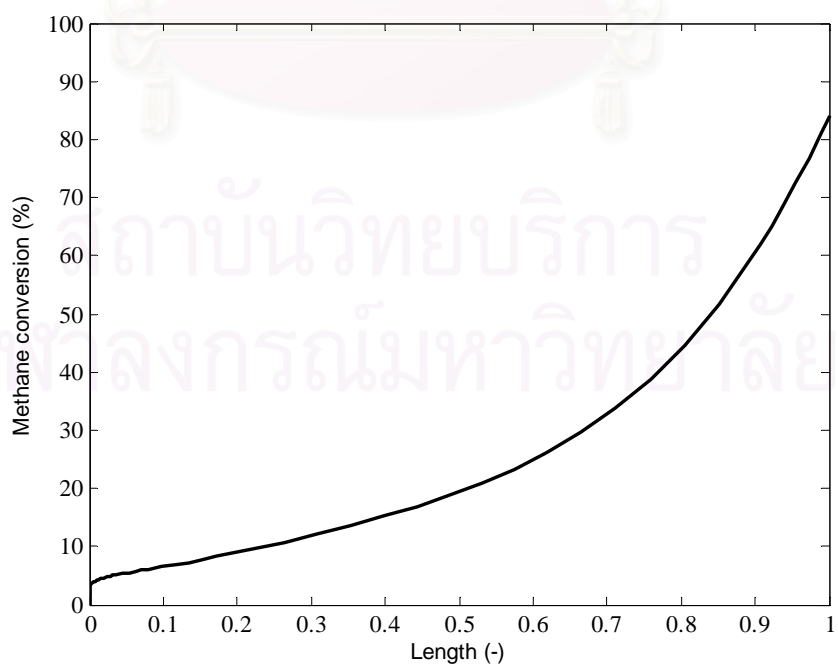


**Figure 5.22** Methane conversion profile of an  $\text{O}_2$ -selective membrane reactor



As oxygen gradually permeates through the membrane to react with methane, the oxidation reaction is balanced by the reforming reaction along the reactor length. As a result of this, the conversion of methane slowly increases. The maximum methane conversion is 84.12 % and the outlet temperature is 1014 K.

#### 5.4.2.1 Effect of H<sub>2</sub>O/CH<sub>4</sub> ratio

Because vapor steam involves the autothermal reforming reaction, the amount of steam may have an impact on the reactor performance. Figure 5.23 shows the effect of H<sub>2</sub>O/CH<sub>4</sub> varied in the range of 0.5-1.5 on the reactor performance in terms methane conversion and outlet temperature. It is found that the methane conversion and the outlet temperature decrease with increasing the H<sub>2</sub>O/CH<sub>4</sub> ratio. More steam in feed promotes the reforming reaction, so that the outlet temperature decreases.

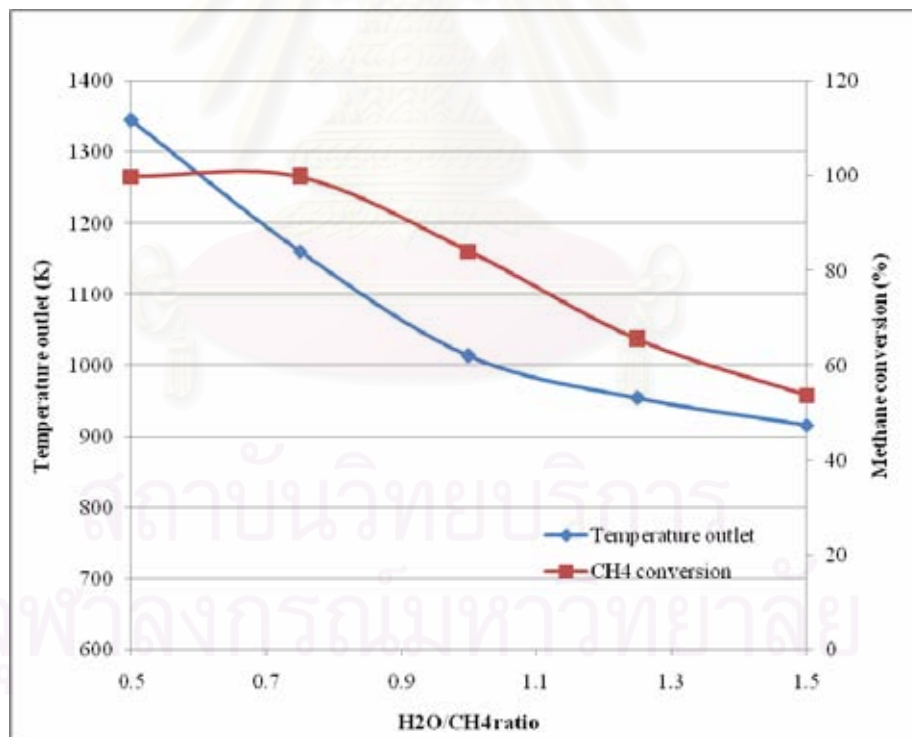


**Figure 5.23** Temperature outlet and CH<sub>4</sub> conversion of an O<sub>2</sub>-selective membrane reactor by varying H<sub>2</sub>O/CH<sub>4</sub> ratio

Table 5.10 presents the result of the  $\text{H}_2\text{O}/\text{CH}_4$  ratio on the  $\text{H}_2/\text{CO}$  ratio of product. Increasing the  $\text{H}_2\text{O}/\text{CH}_4$  ratio increase the  $\text{H}_2/\text{CO}$  ratio of product due to higher rate of steam reforming and water gas shift reaction.

**Table 5.10** Effect of the  $\text{H}_2\text{O}/\text{CH}_4$  ratio and the  $\text{O}_2/\text{CH}_4$  ratio on the  $\text{H}_2/\text{CO}$  ratio of product in  $\text{O}_2$ -selective membrane reactor

$\text{H}_2\text{O}/\text{CH}_4$ ratio	$\text{H}_2/\text{CO}$ of product	$\text{O}_2/\text{CH}_4$ ratio	$\text{H}_2/\text{CO}$ of product
0.50	2.06	0.30	4.22
0.75	2.54	0.50	3.37
1.00	3.37	0.75	3.28
1.25	4.77	1.00	3.26
1.50	6.85	1.25	3.27

#### 5.4.2.2 Effect of $\text{O}_2/\text{CH}_4$

The effect of the  $\text{O}_2/\text{CH}_4$  ratio varied from 0.3 to 1.25 on the reactor performance is shown in Figure 5.24. An increase in the  $\text{O}_2/\text{CH}_4$  results in an increased temperature and in turn the conversion of methane.

#### 5.4.2.3 Effect of the thickness of $\text{O}_2$ -selective membrane

In this section, the effect of the thickness of the  $\text{O}_2$ -selective membrane is studied. The result shows that increasing the membrane thickness from 5  $\mu\text{m}$  to 10  $\mu\text{m}$  decreases the methane conversion as less oxygen can diffuse to the reaction side.

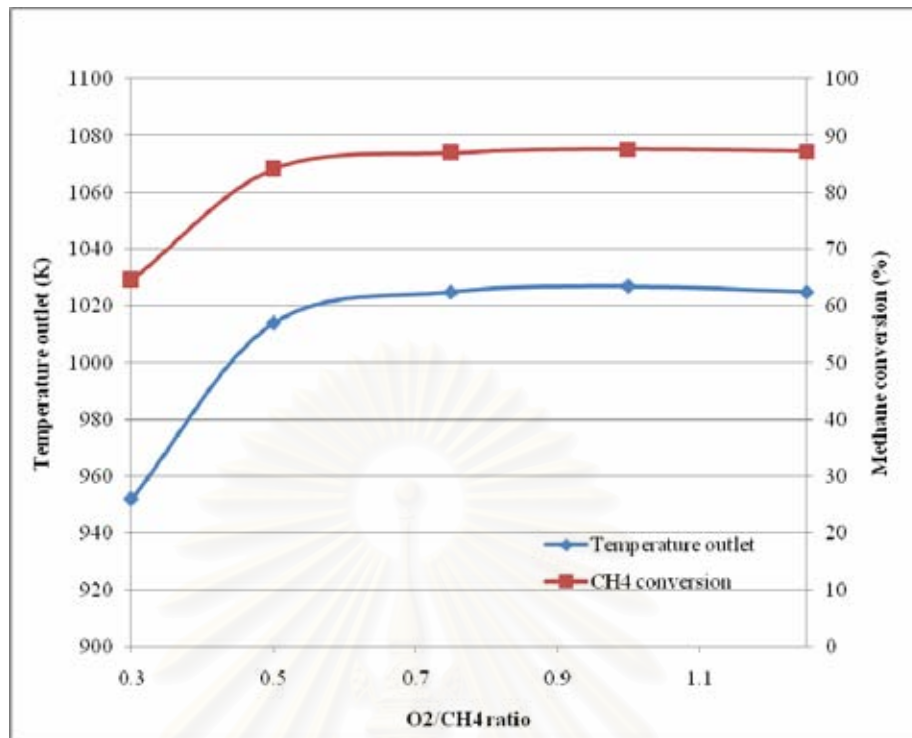


**Figure 5.24** Effect of the O<sub>2</sub>/CH<sub>4</sub> ratio on an O<sub>2</sub>-selective membrane reactor.

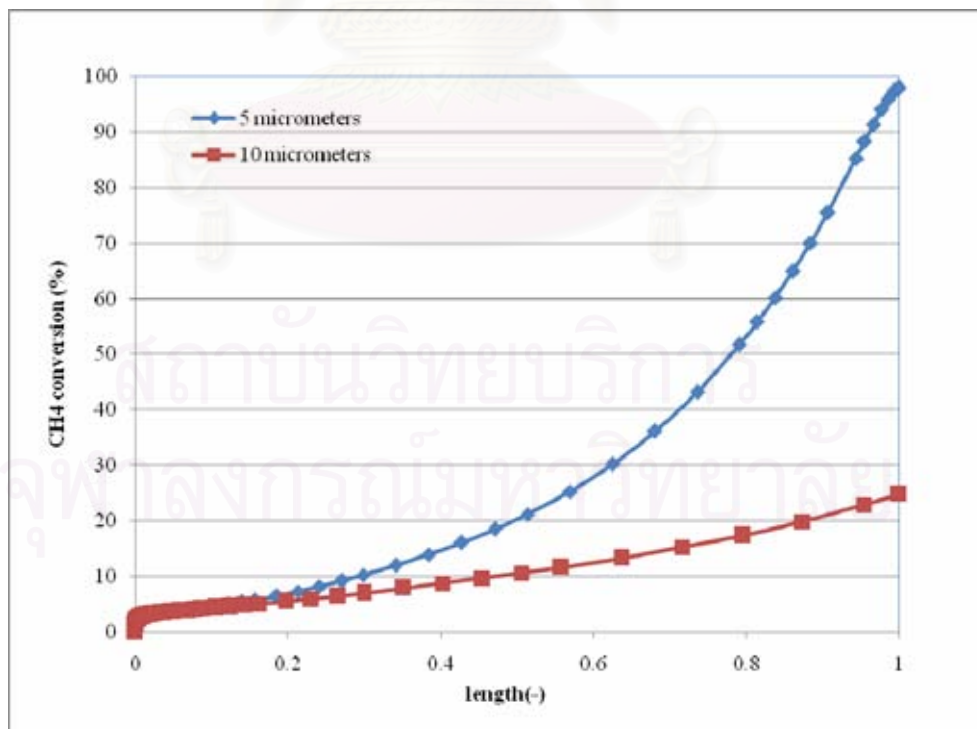


**Figure 5.25** Effect of membrane thickness on an O<sub>2</sub>-selective membrane reactor.

### 5.4.3 H<sub>2</sub>-O<sub>2</sub> selective membrane reactor

From previous section, it is found that the H<sub>2</sub>-selective membrane reactor can improve the reactor performance. Continuous removing hydrogen from the reaction side can shift the equilibrium of reforming reaction and thus, the methane conversion is enhanced. At the same time, higher pure hydrogen is obtained at the permeation side. For O<sub>2</sub>-selective membrane reactor, it is shown that the temperature profile along the reformer is improved and the hot spot is reduced.

In this section, the integration of such two membranes in a single reactor is investigated. The H<sub>2</sub>-O<sub>2</sub> selective membrane reactor is a double jacket reactor as shown in Figure 4.4. Figures 5.26-5.27 respectively shows the temperature and methane conversion profiles when gas feed with the H<sub>2</sub>O/CH<sub>4</sub> ratio of 1.0 and the O<sub>2</sub>/CH<sub>4</sub> ratio of 0.5 is introduced to the reactor. It is seen from Figure 5.27 that the temperature drops sharply at the inlet due to fast endothermic steam reforming reaction. When oxygen permeates to the reaction side, the temperature is increased by the exothermic oxidation reaction. Higher operating temperature increases the rate of steam reforming and oxidation and thus, the conversion of methane is increased as in Figure 5.27. Figure 5.28 shows the gas composition profile of the reactor.

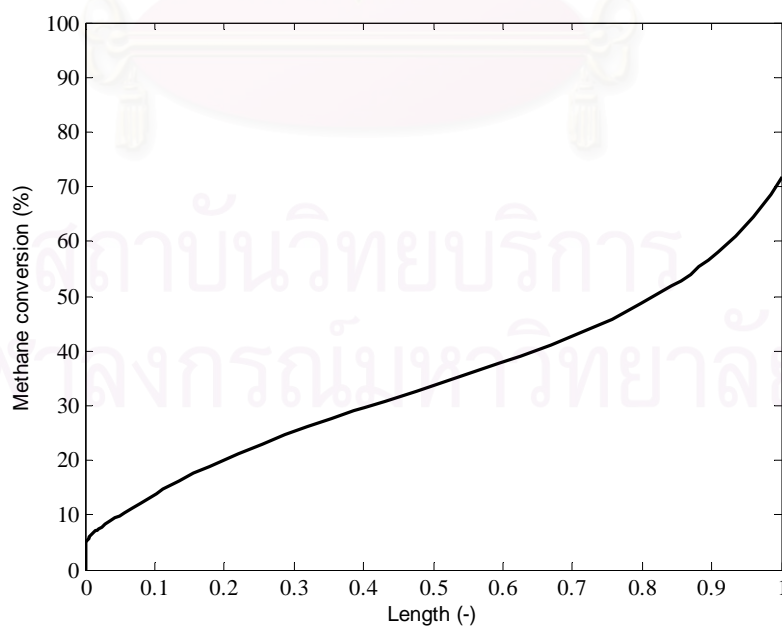


**Figure 5.26** Temperature profile of a H<sub>2</sub>-O<sub>2</sub> selective membrane reactor

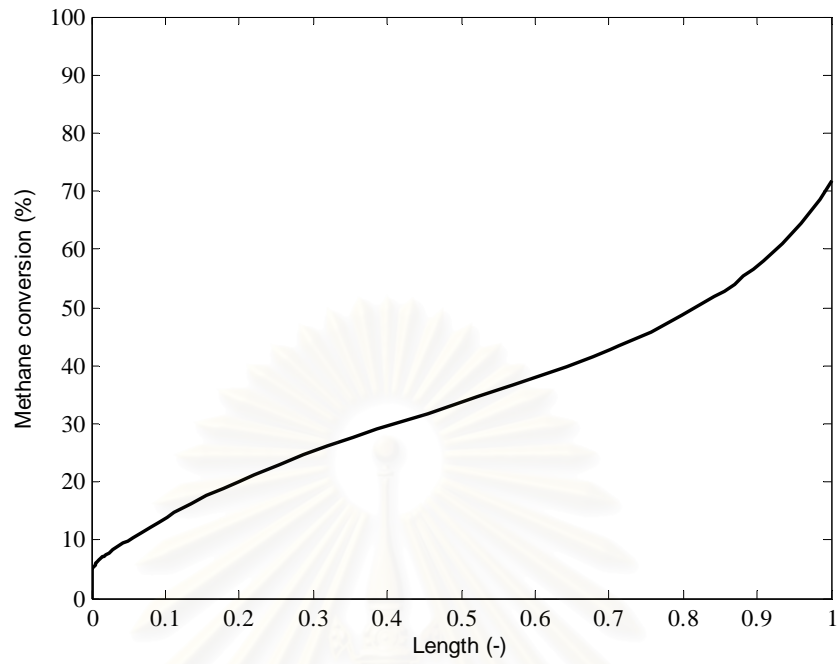


**Figure 5.27** Methane conversion profile of a  $\text{H}_2\text{-O}_2$  selective membrane reactor

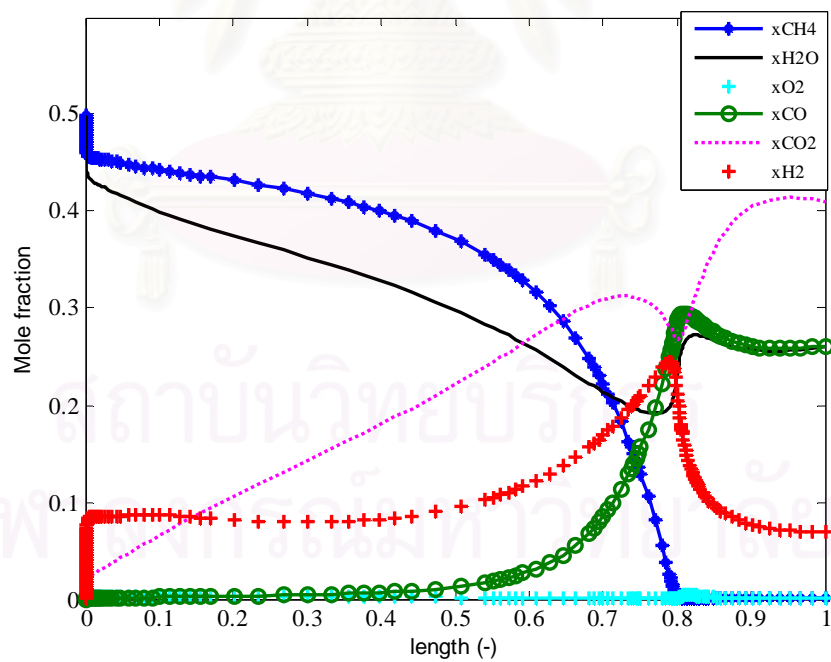


**Figure 5.28** Gas composition profile of a  $\text{H}_2\text{-O}_2$  selective membrane reactor

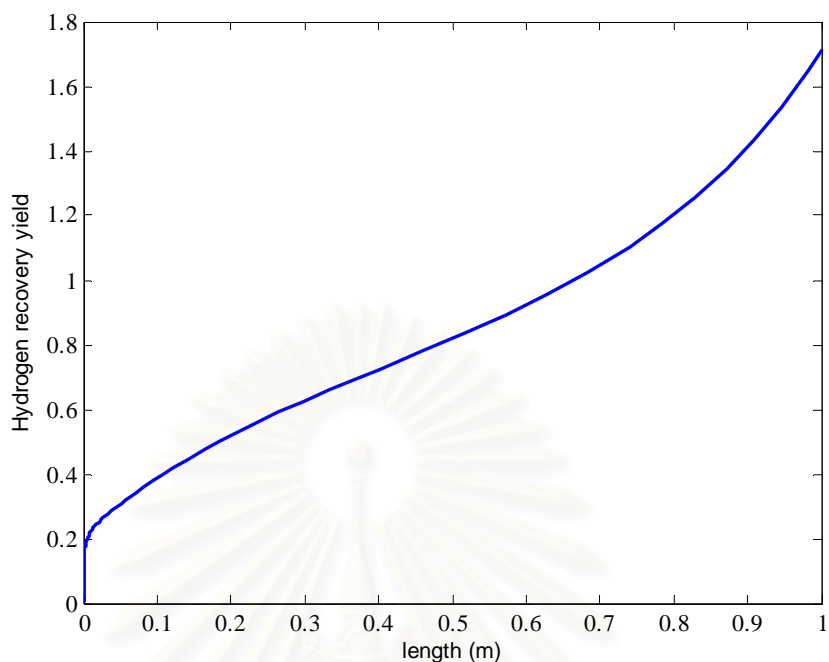
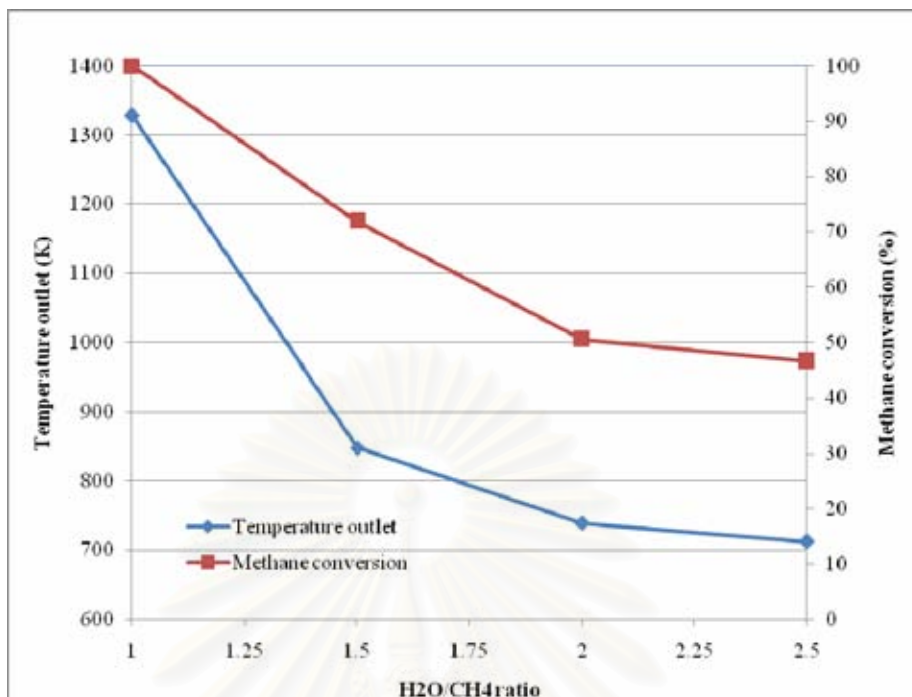


**Figure 5.29** The hydrogen recovery yield profile of a  $H_2$ - $O_2$  selective membrane reactor

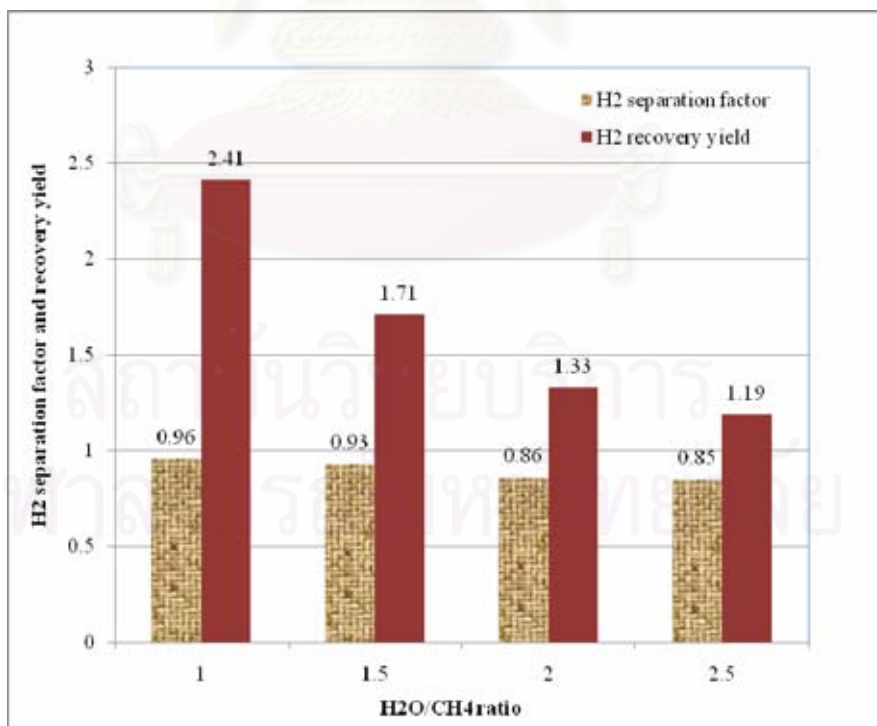
Figure 5.29 illustrates the hydrogen recovery profile of the  $H_2$ - $O_2$  selective membrane reactor. The yield of hydrogen increases along the reactor length. From simulation result, one mole of methane can produce 1.7 model of hydrogen.

#### 5.4.3.1 Effect of $H_2O/CH_4$ ratio

Figure 5.30 shows the effect of the  $H_2O/CH_4$  ratio on the outlet temperature and methane conversion. It is found that the outlet temperatures and the methane conversion decrease against the increased  $H_2O/CH_4$  ratio. Due to high steam in gas feed, more methane steam reforming is performed. Therefore, a decrease in the outlet temperature is observed. As operating temperature decreases, the rate of steam reforming and oxidation is less pronounced and thus the conversion of methane is reduced. In addition, the yield of hydrogen is decreased as can be seen in Figure 5.31.



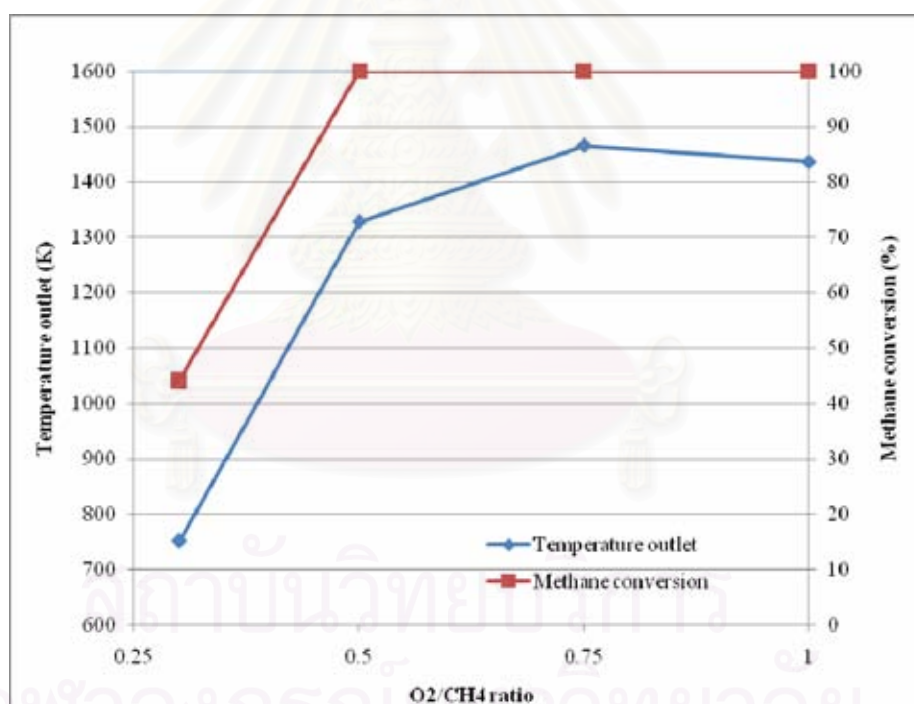
**Figure 5.30** Effect of H<sub>2</sub>O/CH<sub>4</sub> ratio on outlet temperature and methane conversion of an H<sub>2</sub>-O<sub>2</sub> selective membrane reactor.



**Figure 5.31** Effect of H<sub>2</sub>O/CH<sub>4</sub> ratio on H<sub>2</sub> separation factor and recovery yield of a H<sub>2</sub>-O<sub>2</sub> selective membrane reactor.

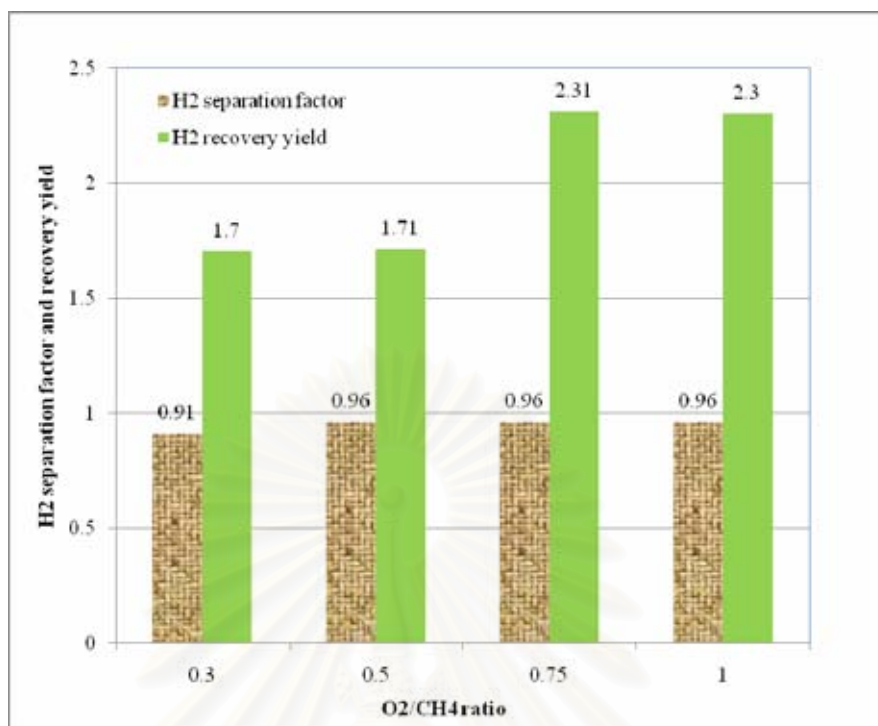
### 5.4.3.2 Effect of O<sub>2</sub>/CH<sub>4</sub> ratio

Figure 5.32 shows the effect of variation of the O<sub>2</sub>/CH<sub>4</sub> ratio on the outlet temperature and the conversion of methane. It is seen that both the outlet temperature and methane conversion increase with increasing the O<sub>2</sub>/CH<sub>4</sub> ratio in feed stream. With an increase of the O<sub>2</sub>/CH<sub>4</sub> ratio, oxygen can increasingly permeate to the reaction side and then the exothermic oxidation highly occurs. Thus, the temperature of the reformer is increased. The increased temperature causes high oxidation reaction and in turn the conversion of methane. The complete conversion of methane is met at the O<sub>2</sub>/CH<sub>4</sub> ratio of 0.5. Figure 5.33 illustrated the effect of varying O<sub>2</sub>/CH<sub>4</sub> ratio on the hydrogen separation factor and hydrogen recovery yield.



**Figure 5.32** Effect of O<sub>2</sub>/CH<sub>4</sub> ratio on the performance of a H<sub>2</sub>-O<sub>2</sub> selective membrane reactor.





**Figure 5.33** Effect of O<sub>2</sub>/CH<sub>4</sub> ratio on the H<sub>2</sub> separation factor and recovery yield of a H<sub>2</sub>-O<sub>2</sub> selective membrane reactor.

#### 5.4.3.3 Effect of air pressure

The effect of air pressure varied between 1-14 bar on the performance of the H<sub>2</sub>-O<sub>2</sub> selective membrane reactor is shown in Figure 5.34. The methane conversion and hydrogen recovery yield show a similar trend; they increase with increasing air pressure. The increased air pressure causes more oxygen permeating to the reaction side, thus promoting methane oxidation. This leads to an increase in the conversion of methane and the yield of hydrogen.

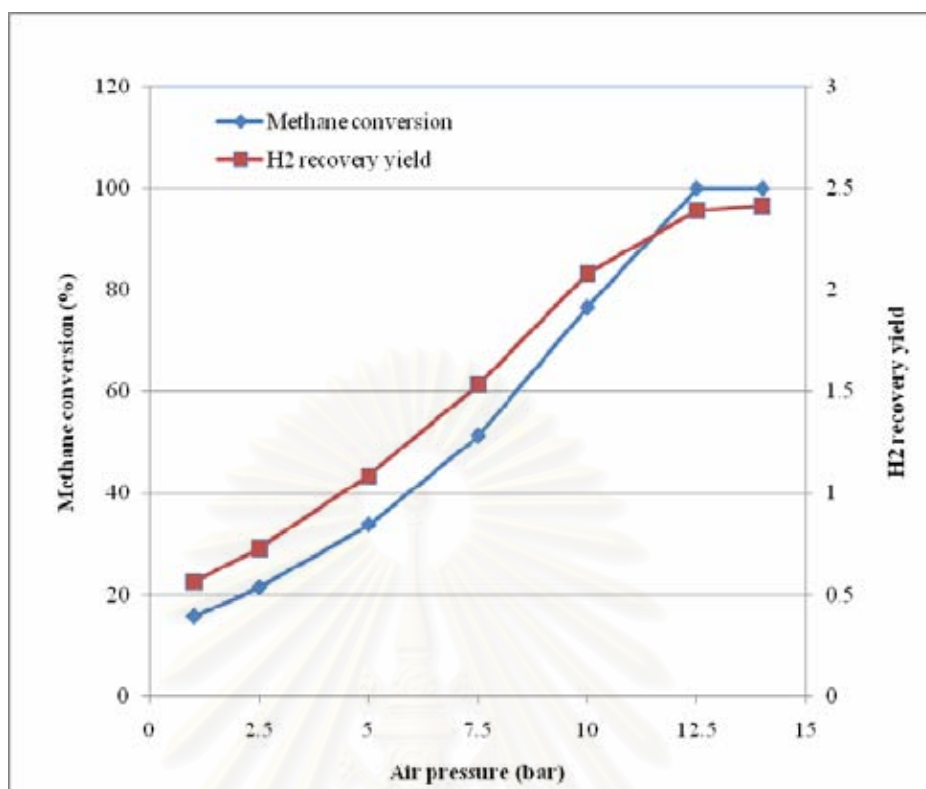


**Figure 5.34** Effect of air pressure on the performance of a H<sub>2</sub>-O<sub>2</sub> selective membrane reactor.

#### 5.4.3.4 Effect of air temperature

The temperature of air involves the permeability of oxygen and reaction rates. In this section the effect of air temperature on the reformer performance is investigated. It is found from Figure 5.35 that an increase in air temperature increases the methane conversion and the hydrogen yield. Higher air temperature causes increases the permeation flux of oxygen through the membrane and thus increasing the methane oxidation.

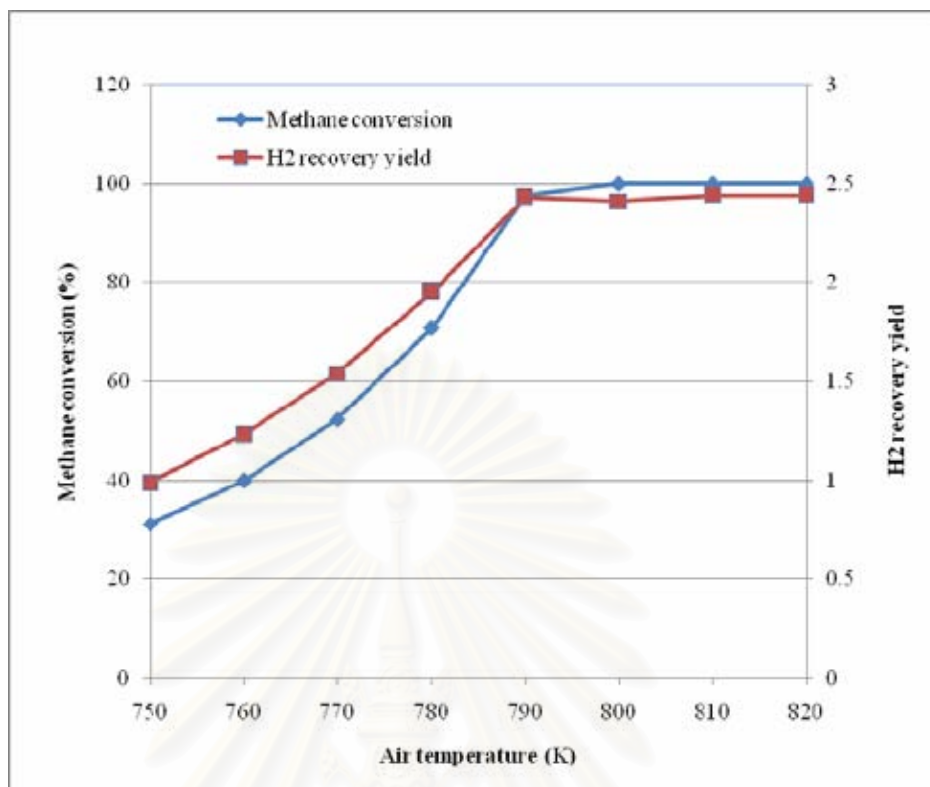


**Figure 5.35** The CH<sub>4</sub> conversion and H<sub>2</sub> recovery yield of a H<sub>2</sub>-O<sub>2</sub> selective membrane reactor by varying air temperature

สถาบันวิทยบริการ  
จุฬาลงกรณ์มหาวิทยาลัย

# CHAPTER VI

## CONCLUSION AND RECOMMENDATIONS

In this study, the performance of three autothermal reactors, i.e., a conventional reactor, a dual bed reactor and a membrane reactor, for the production of hydrogen from methane is analyzed by using a one-dimensional homogeneous and non-isothermal reactor model. Different types of membrane (i.e., H<sub>2</sub>-selective membrane, O<sub>2</sub>-selective membrane, and H<sub>2</sub>-O<sub>2</sub> selective membrane) are applied to the membrane reactors. The obtained results are summarized in the subsequent section.

### 6.1 Conventional autothermal reactor

A conventional autothermal reactor is an adiabatic fixed-bed reactor in which Ni-MgAl<sub>2</sub>O<sub>4</sub> catalysts are packed (Xu and Froment, 1989). The feed stream consisting of methane, steam and air, are introduced to the reactor to carry out reforming reactions of methane as a fuel to produce hydrogen-rich gas.

Simulation of a conventional autothermal reactor fed by methane with the H<sub>2</sub>O/CH<sub>4</sub> ratio of 1.5 and the O<sub>2</sub>/CH<sub>4</sub> ratio of 0.5 at the standard condition shows that the temperature outlet and the methane conversion are 1057 K and 97.81%, respectively. The amount of steam and oxygen has slight effect on the H<sub>2</sub>/CO ratio of product and the methane conversion.

Further, it is found that adding steam at the first part of the reformer ( $z < 0.10$  m.) shows high methane conversion and H<sub>2</sub>/CO ratio of product. The optimum condition that gives the maximum methane conversion and H<sub>2</sub>/CO ratio of product is to add steam of which the temperature is 600K at the reactor position of 0.10 meter. The methane conversion and H<sub>2</sub>/CO ratio of product at this condition are 99.90% and 6.04, respectively.

## 6.2 Dual bed autothermal reactor

The dual bed autothermal reactor considered in this work is a conventional fixed bed reactor that a catalyst bed is separated into two sections. The first section is the oxidation section in which Pt-Al<sub>2</sub>O<sub>3</sub> catalyst is packed whereas the second section involves a steam reforming reaction and is packed with Ni-MgAl<sub>2</sub>O<sub>4</sub> catalyst. A gas mixture of methane, steam and air is fed into the first zone of the reactor to convert fuel into synthesis gas. Then the synthesis gas from the first zone enters the second zone where the steam reforming is carried out to produce hydrogen-rich-gas. It is assumed that the partial oxidation section occupy the reactor volume of 10%.

Compared with the conventional autothermal reactor, the dual bed autothermal reactor provides a better performance in terms of the conversion of methane. However, it is observed that the H<sub>2</sub>/CO ratio of the product gas from the dual bed reactor is lower than that of the conventional reactor. The maximum temperature of the dual bed reactor is higher than that of the conventional reactor due to the unbalance of heat of oxidation and steam reforming reactions

## 6.3 Autothermal membrane reactors

In this section, an autothermal membrane reactor with different types of membrane is studied for the production of hydrogen from methane. The palladium-silver (Pd-Ag) membrane is applied to the reactor as a H<sub>2</sub>-selective membrane for pure hydrogen production. The perovskite ( $La_{0.2}Ba_{0.8}Fe_{0.8}Co_{0.2}O_{3-\delta}$ ) membrane is used as an O<sub>2</sub>-selective membrane for oxygen permeation. Based on such the membrane, three types of the membrane reactor are studied: a H<sub>2</sub>-selective membrane reactor, an O<sub>2</sub>-selective membrane, and a H<sub>2</sub> and O<sub>2</sub> selective membrane reactor.

### 6.3.1 H<sub>2</sub>-selcetive membrane reactor

The H<sub>2</sub>-selective autothermal membrane reactor consists of two concentric tubes. An internal tube is coated with Pd-Ag membrane to allow hydrogen to

permeate from the reaction side to the permeate side to form pure hydrogen production.

When methane at the  $\text{H}_2\text{O}/\text{CH}_4$  ratio of 1.5 and the  $\text{O}_2/\text{CH}_4$  ratio of 0.5 is fed to the reactor at the standard condition, the outlet temperature and the methane conversion are 1060 K and 99.44 %, respectively. At this condition, the maximum hydrogen separation factor  $\alpha_{\text{H}_2}$  and value of hydrogen yield are 0.6 and 2.50, respectively. This shows that the  $\text{H}_2$ -selective membrane reactor can improve the pure hydrogen production and methane conversion.

From an analysis of the reactor, it is found that the  $\text{H}_2\text{O}/\text{CH}_4$  ratio has a slight effect on the methane conversion and the reactor temperature; however, it has a strong effect on hydrogen separation factor as it decreases with increasing the  $\text{H}_2\text{O}/\text{CH}_4$  ratio. The increased  $\text{H}_2\text{O}/\text{CH}_4$  ratio also increases the hydrogen recovery yield. By varying  $\text{O}_2/\text{CH}_4$  ratio of feed, it is found that the methane conversion increases with increasing the  $\text{O}_2/\text{CH}_4$  ratio since oxygen can react with more methane leading to higher methane conversion.

When the reactor is operated under vacuum pressure condition (0.05 bar), the results show that more hydrogen can permeate through the membrane, thus increasing the water shift reaction rate; higher  $\text{CO}_2$  is observed.

### **6.3.2 $\text{O}_2$ -selective membrane reactor**

An autothermal  $\text{O}_2$ -selective membrane reactor is applied to produce hydrogen from methane;  $\text{O}_2$ -selective membrane derived from perovskite membrane is used to control oxygen entering the reaction side.

Simulation performed at the standard condition shows that the reactor temperature steadily increases from the inlet. As oxygen gradually permeates through the membrane to react with methane, the oxidation reaction is balanced by the reforming reaction along the reactor length. As a result of this, the conversion of

methane slowly increases. The maximum methane conversion is 84.12 % and the outlet temperature is 1014 K.

As the  $\text{H}_2\text{O}/\text{CH}_4$  ratio increases, the methane conversion and the outlet temperature decrease but the  $\text{H}_2/\text{CO}$  ratio of product increases. An increase in the  $\text{O}_2/\text{CH}_4$  results in an increased temperature and in turn the conversion of methane. In addition, it is found that increasing the membrane thickness from 5  $\mu\text{m}$  to 10  $\mu\text{m}$  decreases the methane conversion as less oxygen can diffuse to the reaction side.

### 6.3.3 $\text{H}_2\text{-O}_2$ selective membrane reactor

For the study of  $\text{H}_2$ -selective membrane reactor, it provides that continuous removing hydrogen from the reaction side can shift the equilibrium of reforming reaction and thus, the methane conversion is enhanced. At the same time, higher pure hydrogen is obtained at the permeation side. For  $\text{O}_2$ -selective membrane reactor, it is shown that the temperature profile along the reformer is improved and the hot spot is reduced. Therefore, the integration of such two membranes in a single reactor,  $\text{H}_2\text{-O}_2$  selective membrane reactor, should be considered.

From simulation study under the standard condition where the gas feed with the  $\text{H}_2\text{O}/\text{CH}_4$  ratio of 1.0 and the  $\text{O}_2/\text{CH}_4$  ratio of 0.5 is introduced to the reactor, it is shown that the temperature drops sharply at the inlet due to fast endothermic steam reforming reaction. When oxygen permeates to the reaction side, the temperature is increased by the exothermic oxidation reaction. The outlet temperatures and the methane conversion decrease against the increased  $\text{H}_2\text{O}/\text{CH}_4$  ratio. Due to high steam in gas feed, more methane steam reforming is performed. Therefore, a decrease in the outlet temperature is observed. Further, it is noticed that the outlet temperature and methane conversion increase with increasing the  $\text{O}_2/\text{CH}_4$  ratio in feed stream.

Considering the effect of the pressure and temperature of air feed, it is found that an increase in both air pressure and temperature enhances the reactor performance in terms of the methane conversion and hydrogen recovery yield.

## 6.4 Recommendation

As hot spot in a catalyst bed is found in both a conventional and a dual bed autothermal reforming reactor, an optimal design of the reactors should be further studied to solve such a problem. For autothermal membrane reactors, since hydrogen and/or oxygen are permeated through a selective membrane, the effect of mass and heat transfer in a radial direction of the membrane reactors should be investigated in more detail.



สถาบันวิทยบริการ  
จุฬาลงกรณ์มหาวิทยาลัย



## REFERENCES

- Avci, A.K., Trimm, D.L. and Önsan, Z.I., Heterogeneous reactor modeling for simulation of catalytic oxidation and steam reforming of methane. Chemical Engineering Science 56 (2001): 641-649.
- Basile, A., Paturzo, L. and Lagana, F., The partial oxidation of methane to syngas in palladium membrane reactor: Simulation and experimental studies. Catalysis Today 67 (2001): 65-75.
- Basile, A., Gallucci, F. and Paturzo, L., Hydrogen production from methanol by oxidative steam reforming carried out in a membrane reactor. Catalysis Today 104 (2005): 251-259.
- Basile, A., Tereschenko, G.F., Orekhova, N.V., Ermilova, M.M., Gallucci, F. and Paturzo, L., An experimental investigation on methanol steam reforming with oxygen addition in a flat Pd–Ag membrane reactor. International Journal of Hydrogen Energy (2006): 1615-1622.
- Charudatta, S.P., Martin, S.A. and Kuipers, J.A.M., Design of a novel autothermal membrane-assisted fluidized-bed reactor for the production of ultrapure hydrogen from methane. Industrial Engineering Chemical Resources 44 (2005): 9502-9512.
- Chen, Y., Xu, H., Wang, Y. and Xiong, G., Hydrogen production from the steam reforming of liquid hydrocarbons in membrane reactor. Catalysis Today 118 (2006): 136-143.
- Chen, Z. and Elnashaie, S.S.E.H., Autothermal CFB membrane reformer for hydrogen production from heptane. Chemical Engineering Research and Design 83 (A7) (2005): 893-899.
- Chen, Z., Yan, Y. and Elnashaie, S.S.E.H., Hydrogen production and carbon formation during the steam reformer of heptane in a novel circulating fluidized bed membrane reformer. Industrial Engineering Chemical Resources 43 (2004): 1323-1333.
- Christensen, T.S. and Primdahl, I.I., Improve syngas production using autothermal reforming. Hydrocarbon Process 73 (1994): 39-45.

- Dicks, A.L., Hydrogen generation from natural gas for the fuel cell system of tomorrow. Journal of power sources 61 (1996): 113-124.
- Docter, A. and Lamm, A., Gasoline fuel cell systems. Journal of power sources 84 (1999): 1994-2000.
- Ersoz, A., Olgun, H., Ozdogan, S., Gungor, C., Akgan, F. and Tiri, M., ATR as a hydrocarbon fuel processing option for PEM fuel cell. Journal of power sources 118 (2003): 384-392.
- Ferreira, A.P., Benito, M., Kouachi, K. and Menad, S., Catalysis in membrane reformers: a high-performance catalytic system for hydrogen production from methane. Journal of catalysis 231(2) (2005): 331-343.
- Freni, S., Calogero, G. and Cavallaro, S., Hydrogen production from methane through catalytic partial oxidation reactions. Journal of power sources 87 (2000): 28-38.
- Fukuhara, C. and Igarashi, A., Performance simulation of a wall-type reactor in which exothermic and endothermic reactions proceed simultaneously, comparing with that of a fixed-bed reactor. Chemical Engineering Science 60 (2005): 6824-6834.
- Gadhe, J.B. and Gupta, R.B., Hydrogen production by methanol reforming in supercritical water: suppression of methane formation. Industrial Engineering Chemical Resources 44 (2005): 4577-4585.
- Groote, A.M. and Froment, G.F., Simulation of the catalytic partial oxidation of methane to synthesis gas. Applied Catalysis A: General 138 (1996): 245-264.
- Halabi, M.H., Croon, M.H.J.M., Schaaf, J., Cobden, P.D. and Schouten, J.C., Modeling and analysis of autothermal reforming of methane to hydrogen in a fixed bed reformer. Chemical Engineering Journal xxx (2007): xxx-xxx.
- Hoang, D.L. and Chan, S.H., Modeling of a catalytic autothermal methane reformer for fuel cell applications. Applied Catalysis A: General 268 (2004): 207-216.
- Hoang, D.L., Chan, S.H. and Ding, O.L., Hydrogen production for fuel cells by autothermal reforming of methane over sulfide nickel catalyst on a gamma alumina support. Journal of Power Sources 159 (2006): 1248-1257.
- Ji, P., Kooi, H.J. and Arons, J.S., Simulation and thermodynamic analysis of an integrated process with H<sub>2</sub> membrane CPO reactor for pure H<sub>2</sub> production. Chemical Engineering Science 58 (2003): 3901-3911.

- Ji, P., Kooi, H.J. and Arons, J.S., Simulation and thermodynamic analysis of conventional and oxygen permeable CPO reactors. Chemical Engineering Science 58 (2003): 2921-2930.
- Julbe, A., Farrusseng, D. and Guizard, C., Porous ceramic membranes for catalytic reactors—overview and new ideas. Journal of Membrane Science 181 (2001): 3-20.
- Kikuchi, E., Membrane reactor application to hydrogen production. Catalysis Today 56 (2000): 97-101.
- Kumar, R., Barge, S., Kulkarni, P., Moorefield, C. and Zamansky, V., Autothermal cyclic reforming based hydrogen generating and dispensing system. Hydrogen. Fuel Cells and Infrastructure Technologies. Progress Report (2003).
- Kolios, G., Frauhammer, J. and Eigenberger, G., A simplified procedure for the optimal design of autothermal reactors for endothermic high-temperature reactions. Chemical Engineering Science 56 (2001): 351-357.
- Kolios, G., Frauhammer, J. and Eigenberger, G., 2002. Efficient reactor concepts for coupling of endothermic and exothermic reactions. Chemical Engineering Science 57 (2002): 1505-1510.
- Lattner, J.R. and Harold, M.P., Autothermal reforming of methanol: Experiments and modeling. Catalysis Today 120 (2007): 78-89.
- Lattner, J.R. and Harold, M.P., Comparison of conventional and membrane reactor fuel processors for hydrocarbon-based PEM fuel cell systems. International Journal of Hydrogen Energy 29 (2004): 393-417.
- Lin, Y.M. and Rei, M.H., Study on the hydrogen production from methanol steam reforming in supported palladium membrane reactor. Catalysis Today 67 (2001): 77-84.
- Ma, L., Jiang, C., Adesina, A.A., Trimm, D.L. and Wainwright, M.S., Simulation studies of autothermal reactor system for H<sub>2</sub> production from methanol steam reforming. Chemical Engineering Journal & the Biochemical Engineering Journal 62 (1996): 103-111.
- Ma, L., Trimm, D.L. and Jiang, C., The design and testing of an autothermal reactor for the conversion of light hydrocarbons to hydrogen I. The kinetics of the

- catalytic oxidation of light hydrocarbons. Applied Catalysis A: General 138 (1996): 275-283.
- Madia, G.S., Barbieri, G. and Drioli, E., Theoretical and experimental analysis methane steam reforming in a membrane reactor. Chemical Engineering Journal 77 (1999): 698-706.
- Marsh, H. and Thiagarajan, T., AIChE Ammonia Safety Symp (1992).
- Ohmori, T., Yu, W.F., Yamamoto, T., Endo, A., Nakaiwa, M. and Itoh, N., Simulation study on ceramic membrane reactor for hydrogen production. Journal of the Chinese Institute of Engineers 28 (7) (2005): 1069-1075.
- Qi, A., Peppley, B. and Karan, K., Integrated fuel processors for fuel cell application: A review. Fuel Processing Technology 88 (2006): 3-22.
- Peña, M.A., Gomez, G.P. and Fierro, J.L.G., New catalytic routes for syngas and hydrogen production. Applied catalysis A: General 144 (1996): 7-57.
- Peppley, B.A., Amphlett, J.C., Kearns, L.M. and Mann, R.F., Methanol-steam reforming on Cu/ZnO/Al<sub>2</sub>O<sub>3</sub> catalysts. Part 2. A comprehensive kinetic model. Applied Catalysis. A: General 179 (1999): 31-49
- Sanger, R.J., Bussche, K.M.V. and Sioui, D.R., US6793698B1 (2004).
- Schwartz, J., Apte, P., Drnevich, R. and Damle, A., DOE Hydrogen Program. Progress Report 18 (FY2004).
- Tiemersma, T.P., Patil, C.S., Annaland, M.S. and Kuipers, J.A.M., Modelling of packed bed membrane reactors for autothermal production of ultrapure hydrogen. Chemical Engineering Science 61 (2006): 1602-1616.
- Tong, J. and Matsumura, Y. Pure hydrogen production by methane steam reforming with hydrogen-permeable membrane reactor. Catalysis Today 111 (2005): 147-152.
- Trimm, D.L. and Lam, C.-W., The combustion of methane on platinum-alumina fiber catalysts-I. Kinetics and mechanism. Chemical Engineering Science 35 (1980): 1405-1413.
- Tsai, C., Dixon, A.G., Moser, W.R. and Ma, Y.H., Dense perovskite membrane reactors for partial oxidation of methane to syngas. AIChE Journal. Ceramic Processing Vol. 43, No. 11A (1997): 2741-2750.

- Tsai, C., Ma, Y.H., Moser, W.R. and Dixon, A.G., Modelling and simulation of a nonisothermal catalytic membrane reactor. Chemical Engineering Communications 134 (1995): 107-132.
- Vernon, P.D.F., Green, M.L.H., Cheetham, A.K. and Ashcroft, A.T., Partial oxidation of methane to synthesis gas, and carbon dioxide as an oxidizing agent for methane conversion. Catalysis Today 13 (1992): 417-426.
- Wang, H.M., Experimental studies on hydrogen generation by methane autothermal reforming over nickel based catalyst. Journal of Power Sources 177 (2008): 506-511.
- Xu, J. and Froment, G.F., Methane steam reforming, Methanation and water gas shift: I-Intrinsic kinetics. AIChE J. 35(1) (1989): 88-96.
- Yoshida, K., Hirano, Y., Fujii, H., Tsuru, T. and Asaeda, M., An application of silica-zirconia membrane for hydrogen separation to membrane reactor. Kagaku Kogaku Ronbunshu 27 (5) (2001): 657-660.
- Yu, W., Ohmori, T., Yamamoto, T., Endo, A., Nakaiwa, M., Hayakawa, T. and Itoh, N., Simulation of a porous ceramic membrane reactor for hydrogen production. International Journal of Hydrogen 30 (10) (2005): 1071-1079.
- Zhixiang, L., Zongqiang, M., Jingming, X., Hess, M.N. and Schmidt, V.M., Operation conditions optimization of hydrogen production by propane autothermal reforming for PEMFC application. Chinese Journal Chemical Engineering 14(2) (2006): 259-265.
- Zhu, W., Han, W., Xiong, G. and Yang, W., Mixed reforming of simulated gasoline to hydrogen in a BSCFO membrane. Catalysis Today 118 (2006): 39-43.



**APPENDIX**

สถาบันวิทยบริการ  
จุฬาลงกรณ์มหาวิทยาลัย

## APPENDIX A

### LIST OF PUBLICATIONS

#### National conference

1. Manatsanan Wasuleewan and Amornchai Arpornwichanop. Performance analysis of an autothermal reactor for hydrogen production from methane. The 17th Thailand Chemical Engineering and Applied Chemistry Conference, Chiangmai, Thailand, Oct. 29-30, 2007: EFF16\_1-4 (IN THAI).



สถาบันวิทยบริการ  
จุฬาลงกรณ์มหาวิทยาลัย

## VITA

Miss Manatsanan Wasuleewan was born in Phatthalung, Thailand on October 28, 1983. She received Bachelor's degree of Engineering from the department of Chemical Engineering, Faculty of Engineering, Prince of Songkla University, Songkhla, Thailand in 2006 and completed Master's degree of Engineering from the department of Chemical Engineering, Faculty of Engineering, Chulalongkorn University, Bangkok, Thailand in 2008.



สถาบันวิทยบริการ  
จุฬาลงกรณ์มหาวิทยาลัย